



# Spontaneous imbibition of modified salinity brine into different lithologies: an improvement of comprehensive scaling used for fractured reservoir simulation

Seyed Mojtaba Bassir<sup>1</sup> · Hassan Shokrollahzadeh Behbahani<sup>1</sup> · Khalil Shahbazi<sup>1</sup> · Shahin Kord<sup>1</sup>

Received: 24 July 2023 / Accepted: 13 January 2024  
© The Author(s) 2024

## Abstract

Spontaneous water imbibition into matrix blocks can be a significant oil recovery mechanism in fractured reservoirs. Many enhanced oil recovery methods, such as injection of modified salinity brine, are proposed for improving spontaneous imbibition efficacy. Many scaling equations are developed in the literature to predict spontaneous imbibition oil recovery. However, almost none of them included the impact of the diversity in ionic composition of injected and connate brines and the blending/interaction of a low salinity imbibing brine with a higher salinity connate brine. In this research, these two issues are included to propose new scaling equations for the scaling of spontaneous imbibition oil recovery by modified salinity imbibing brines. This study uses experimental data of the spontaneous imbibition of modified salinity brines into oil-saturated rock samples with different lithologies containing an irreducible high salinity connate brine. The collected tests from the literature were performed at high temperatures and on aged altered wettability cores. The results of 110 available spontaneous imbibition laboratory experiments (85, 12 and 13 tests on chalks, dolomites and sandstones, respectively) are gathered. This research initially shows the poor ability of three selected convenient scaling equations from the literature to scale imbibition recovery by modified salinity brine. Then, our newly proposed technique to find the scaling equation for spontaneous imbibition recovery by modified salinity brine, during the abovementioned conditions in limestones (Bassir et al. in *J Pet Explor Prod Technol* 13(1): 79–99, 2023. <https://doi.org/10.1007/s13202-022-01537-7>) is used in chalks, dolomites and sandstones to develop the three new scaling equations. Finally, a new general equation to scale imbibition recovery by modified salinity brine for all four lithologies is presented. Moreover, for each of the four datasets (chalk, dolomite, sandstone and all the four lithologies), the scaled data by the new equations is matched by two mathematical expressions based on the Aronofsky et al. model and the Fries and Dreyer model. These mathematical expressions can be used to develop transfer functions in reservoir simulators for a more accurate prediction of oil recovery by spontaneous imbibition of modified salinity brine in fractured reservoirs.

**Keywords** Spontaneous imbibition · Scaling equation · Modified salinity brine · Limestone · Chalk · Dolomite · Sandstone · Enhanced oil recovery · Fractured reservoir simulation

## List of symbols

### English letters

°API Degrees API (American Petroleum Institute)  
 $A$  Surface area (cm<sup>2</sup>)

$a$  A matching parameter in Lambert's  $W$ -function  
AFO All faces open  
 $c$  Molar concentration (mol/L)  
 $C_s$  Salt concentration (ppm)  
COCSI Co-current spontaneous imbibition  
COUCSI Counter-current spontaneous imbibition  
 $D$  Core diameter (cm)  
 $e$  Euler's number  
 $I$  Ionic strength (mol/L)  
IFT Interfacial tension (mN/m)  
IOIP Initial oil in place (cm<sup>3</sup>)  
 $k$  Rock permeability (mD)

✉ Seyed Mojtaba Bassir  
s.m.bassir@put.ac.ir; smb0144@gmail.com

✉ Hassan Shokrollahzadeh Behbahani  
shokrollahzadeh@put.ac.ir

<sup>1</sup> Department of Petroleum Engineering, Ahwaz Faculty of Petroleum Engineering, Petroleum University of Technology (PUT), Ahwaz, Iran

$L$	Core length (cm)
$l_A$	Distance from the imbibition face to the corresponding no-flow boundary (cm)
$L_c$	Characteristic length (cm)
$N$	The empirical exponent in the new scaling equations
$n$	Total number of cases (in Sigma function)
OEO	One end open
$P$	Pressure (psia)
$P_s$	Saturation pressure (psia)
PDI	Potential determining ions
$R$	Oil production (Fraction of IOIP)
$R_\infty$	Ultimate oil recovery (Fraction of IOIP)
RMSE	Root of mean square error
$T$	Temperature ( $^{\circ}\text{C}$ )
$t$	Time (Days)
$t_D$	Dimensionless time
$t_{D\text{-New}}$	New dimensionless time
$t_{\text{end}}$	Total time of recovery (Days)
TAN	Total acid number (mgKOH/g-oil)
tanh	Hyperbolic tangent
TEC	Two ends closed
TEO	Two ends open
$V_b$	Bulk volume ( $\text{cm}^3$ )
$W$	Lambert's $W$ -function
$x$	An arbitrary value between $-e^{-1}$ and zero
$x_{\text{actual}}$	Actual value of each data point
$x_{\text{predicted}}$	The predicted value of each data point
$z$	Charge number

#### Greek letters

$\gamma$	Specific gravity
$\lambda$	Oil production decline constant
$\mu$	Viscosity (cp)
$\sigma$	Interfacial tension (mN/m)
$\varphi$	Rock porosity (Fraction)

#### Subscripts

$i$	$i$ -th case (in Sigma function)
MFMR	Mason, Fischer, Morrow and Ruth
MK	Mattax and Kyte
MMZ	Ma, Morrow and Zhang
o	Oil
od	Dead oil
pw	Pure water
$w$	Imbibing brine
$w_i$	Connate brine

## Introduction

Conventional reservoirs' oil recovery varies from field to field, but the global oil recovery factor is at an average range of 30–35% of the initial oil in place (IOIP) (Aadnoy and

Looyeh 2019). It has been estimated that about 40% of the world's known oil reserves are held in naturally fractured reservoirs. A major portion of the oil reserves in Iran is placed in fractured carbonate formations, such as Asmari, Ilam and Sarvak formations. The biggest oil fields in Iran produced from the formations mentioned above are the Ahwaz, Marun, Aghajari, Gachsaran and Karanj fields (Saidi 1987). High-conductive, low-porosity fractures surround the low-permeability matrix blocks in these reservoirs (Gilman and Kazemi 1983; Mehran Pooladi-Darvish and Abbas Firoozabadi 2000a, b).

Spontaneous imbibition is the crucial mechanism for oil recovery from the matrix blocks located in the water-invaded zone of fractured reservoirs (Aronofsky et al. 1958; Behbahani et al. 2006; Kazemi et al. 1992; Pooladi-Darvish and Firoozabadi 2000a, b; Warren and Root 1963). At the early production times in fractured reservoirs, oil is produced from fractures only; but after a while, the matrix system feeds oil into the fracture network. Oil production from the reservoir continues depending on natural reservoir properties and active drives; however, a large amount of oil could remain at the end of primary recovery (Saidi 1987; van Golf-Racht 1982).

Many enhanced oil recovery (EOR) methods are suggested, such as gas injection (e.g., hydrocarbon gases, inert gases and carbon dioxide), thermal injection (e.g., steam, hot water and combustion) and chemical injection (e.g., nanofluids, ionic liquids, alkalines, surfactants and polymers). Most chemical EOR techniques are used for wettability alteration of reservoir rocks (Bassir and Shadizadeh 2020; Mandal 2015; Salih et al. 2016). Carbonate rocks are usually oil-wet; therefore, wettability alteration towards a relatively water-wet state can diminish the capillary barrier (Chandrasekhar and Mohanty 2013; Das et al. 2021; Standnes 2004; Standnes et al. 2002; Strand et al. 2003).

Modified salinity brine injection is an inexpensive technique that has attracted attention in the last decade. In this strategy, a brine with a lower salinity than the connate brine, with/without manipulation of ionic composition, is injected into the reservoir (Zhang et al. 2006). This technique can be applied individually or hybridly by any chemical EOR method. Recent studies have shown that manipulating the chemistry of injected brine leads to a change in the wettability behavior of the reservoir rock (Chandrasekhar and Mohanty 2013; Kazankapov 2014; Roostaei 2014).

Before the field application, the simulation of the spontaneous imbibition of modified salinity brine into the matrix blocks helps to predict the degree of oil recovery improvement by this technique. Proper scaling equations can improve the simulation accuracy of this process in fractured reservoirs (Behbahani et al. 2006). Scaling equations are dimensionless times considering many variables, including

rock absolute permeability and porosity, the interfacial tension between imbibing brine and oil, the core sample's dimensions, the fluids' viscosities and the boundary conditions. The scaling of spontaneous imbibition recovery data is important in predicting oil recovery from matrix blocks in the water invaded zone of fractured reservoirs (Aronofsky et al. 1958; Kazemi et al. 1992; Ma et al. 1995, 1997; Rapoport 1955; Saidi 1987; van Golf-Racht 1982; Zhang et al. 1996).

Many authors have investigated the effective parameters on spontaneous imbibition efficiency and their configuration in the dimensionless time terms (scaling equations) (Ma et al. 1997; Mason et al. 2010; Mattax and Kyte 1962). Up to now, only Bassir et al. (2023) scaling equation has been suggested (specialized for limestones) to consider the effect of the spontaneous imbibition of a modified salinity imbibing brine into a rock containing higher salinity connate brine. This scaling equation was verified by 59 tests, which were collected from the literature (Bassir et al. 2023).

For this study, 110 spontaneous imbibition experiments by modified salinity brine available in the literature (85, 12 and 13 tests performed on chalk, dolomite and sandstone rock samples, respectively) are collected. At first, three convenient scaling equations are selected and evaluated by the gathered tests to choose the equation with a better scaling quality of data for each lithology. Then, a dimensionless term according to theoretical implications is added to the selected scaling equations to improve them for the scaling imbibition recovery of modified salinity brines. This technique proposes three new scaling equations for chalks, dolomites and sandstones. In the next step, the scaled data by the new scaling equations is matched by two mathematical expressions similar to the Aronofsky et al. model and the Fries and Dreyer model (Aronofsky et al. 1958; Fries and Dreyer 2008). Finally, a universal empirical scaling equation is also presented for all lithology (i.e., limestone (data from our past work (Bassir et al. 2023)), chalk, dolomite and sandstone). Moreover, the two aforementioned mathematical expressions matched this scaled data.

## Fractured reservoirs characteristics

A fractured system consists of two particular media responsible for the fluids' storage and conductance: matrix blocks and fracture networks, respectively (Gilman and Kazemi 1983; van Golf-Racht 1982; Warren and Root 1963). The ultimate oil recovery and spontaneous imbibition rate of each matrix block depend on the properties of each system constituent, such as oil, rock, imbibing and connate brines, in addition to their mutual properties. Moreover, the block's shape and size and the system's boundary condition are other influential factors controlling spontaneous imbibition oil recovery (Hatiboglu and Babadagli 2004; Kazemi et al. 1992).

There are two types of spontaneous imbibition: co-current (COCSI) and counter-current (COUCSI). In the COCSI, the flow directions of displaced and displacing phases are similar, whereas, in the COUCSI, they have contrary directions (Mirzaei-Paiaman et al. 2017; Pooladi-Darvish and Firoozabadi 2000a, b). Most laboratory spontaneous imbibition tests are executed on cylindrical cores saturated with oil and in contact with freshwater/brine in one or more outer surfaces. (Anderson 1986; Fischer et al. 2008). For representing the COUCSI and COCSI, four boundary conditions exist which are all faces open (AFO), one end open (OEO), two ends open (TEO), and two ends closed (TEC) (Fischer et al. 2008; Hatiboglu and Babadagli 2006).

## Scaling equations

The oil recovery factor is the ratio of the amount of the expelled oil from the porous media (e.g., rock sample) to the IOIP. This quantity can also be expressed concerning the pore volume, but it is usual to define the oil recovery factor in terms of IOIP (in ratio or percent). When the oil production ceases, we have touched the ultimate oil recovery ( $R_\infty$ ). The scaling purpose of scattered recovery data is to reach a universal curve of recoverable oil versus dimensionless time in a semi-log plot for all rock/fluid conditions. Recoverable oil is described as the volume of produced oil as a fraction of  $R_\infty$  (Bassir et al. 2023).

Mattax and Kyte (1962) used Rapoport's equation (Rapoport 1955) to scale two tests on sandstone cores and four on alundum cores on two separate plots. They offered the following equation (Mattax and Kyte 1962):

$$t_{D-MK} = t \sqrt{\frac{k}{\phi}} \frac{\sigma}{L^2} \frac{1}{\mu_w} \quad (\text{MK} = \text{Mattax and Kyte}) \quad (1)$$

where  $t$ ,  $k$ ,  $\phi$ ,  $\sigma$ ,  $L$  and  $\mu_w$  are imbibition recovery time, rock absolute permeability, rock porosity, interfacial tension (IFT) between imbibing brine and crude oil, the length of the core and the viscosity of the imbibing brine, respectively (Mattax and Kyte 1962).

Ma et al. (1997) modified Mattax and Kyte's scaling equation. They found that poor definitions of boundary condition and viscosity are the two causes for the simultaneous scaling failure of Mattax and Kyte's equation for recovery data in sandstone and alundum cores. The developed scaling equation by Ma et al. is as follows (Ma et al. 1997):

$$t_{D-MMZ} = t \sqrt{\frac{k}{\phi}} \frac{\sigma}{L_c^2} \frac{1}{\sqrt{\mu_w \mu_o}} \quad (\text{MMZ} = \text{Ma, Morrow, and Zhang}) \quad (2)$$

In Eq. (2), core length ( $L$ ) and viscosity of the imbibing brine ( $\mu_w$ ) in Mattax and Kyte's equation are substituted by a characteristic length ( $L_c$ ) and the geometric mean of

viscosities ( $\sqrt{\mu_w \mu_o}$ ) of crude oil ( $\mu_o$ ) and imbibing brine ( $\mu_w$ ), respectively. The characteristic length includes the effect of various boundary conditions and is defined by (Ma et al. 1997):

$$L_c = \sqrt{\frac{V_b}{\sum_{i=1}^n \frac{A_i}{L_{A_i}}}} \quad (3)$$

where  $V_b$  is the bulk volume of the matrix block,  $A_i$  is the  $i$ -th surface area that is open to flow and  $L_{A_i}$  is the length of the  $i$ -th imbibition face to the no-flow boundary. For an AFO boundary condition and a cylindrical core, the characteristic length is:

$$L_c = \frac{LD}{2\sqrt{D^2 + 2L^2}} \quad (4)$$

where  $D$  and  $L$  are the cylindrical core's diameter and length (height) (Ma et al. 1997).

Mason et al. (2010) suggested a more general scaling equation to scale spontaneous imbibition tests with a broader range of viscosity ratio ( $0.008 < \frac{\mu_o}{\mu_w} < 173$ ). Their scaling equation is (Mason et al. 2010):

$$t_{D-MFMR} = t \sqrt{\frac{k}{\varphi}} \frac{\sigma}{L_c^2} \frac{2}{\mu_w + \sqrt{\mu_w \mu_o}} \quad (\text{MFMR} = \text{Mason, Fischer, Morrow and Ruth}) \quad (5)$$

Table 1 summarizes all the effective parameters of crude oil/brine/rock systems of the spontaneous imbibition tests scaled by the three abovementioned scaling equations, the collected tests of our past work (Bassir et al. 2023) and this study.

Other scaling equations in the literature cannot be used in this study, because some of them need relative permeability and capillary pressure data that were not available (Behbahani and Blunt 2005; Li and Horne 2005, 2006; Mirzaei-Paiaman et al. 2017; Schmid and Geiger 2012, 2013; Standnes and Andersen 2017; Zhou et al. 2002) and some others are developed for the COCSI conditions that are not within the scope of this study (Cai et al. 2012, 2010; Mirzaei-Paiaman et al. 2017; Mirzaei-Paiaman and Masih 2014). Therefore, the scaling equations of Mattax and Kyte, Ma et al. and Mason et al. are selected as the base equations to improve due to the relative similarity of their tests conditions to the experimental data collected for this study.

### Mechanisms of oil recovery improvement by modified salinity imbibing brine

The oil reservoirs usually have a pH level in the acidic range because of the presence of acidic components in the crude oil. In this situation, the charge of the rock surface

in carbonate rocks becomes positive; whereas in sandstone rocks, it is negative (Madsen and Ida 1998; Skauge et al. 1999). During a carbonate rock sample aging in the laboratory, organic acids adsorption from the negatively charged head ( $\text{RCOO}^-$ ) on the rock surface with a positive charge becomes the critical mechanism of carbonate rocks' wettability alteration from a water-wet state to a mixed-/oil-wet state (Fathi et al. 2011a; Fathi et al. 2010a, b).

Wettability alteration by multi-ion exchange with electrical double-layer expansion is believed to be the primary mechanism of oil recovery improvement by modified salinity brine (Shirazi et al. 2020). There are two layers around any charged particle: diffused and stern layers filled with a low- and high-density concentration of ions, respectively (Ligthelm et al. 2009). Due to reducing the imbibing brine salinity, the rock surface's electrical double-layer will be enlarged, and the multi-ion exchange will be boosted. Multivalent ions such as magnesium ( $\text{Mg}^{2+}$ ), calcium ( $\text{Ca}^{2+}$ ) and sulfate ( $\text{SO}_4^{2-}$ ) are considered potential determining ions (PDIs) in the research area of modified salinity brine. These ions are the major contributors to the multi-ion exchange, so that  $\text{Mg}^{2+}$  and  $\text{Ca}^{2+}$  have operative roles while  $\text{SO}_4^{2-}$  has a catalyst role (Fathi et al. 2010a, b).

$\text{Mg}^{2+}$  and  $\text{Ca}^{2+}$  ions can adsorb carboxylic acids (with a negative charge) and separate them from the rock's surface; in this situation, a surface with a positive charge can behave as an obstacle. Mixing a low salinity imbibing brine with a high salinity connate brine will enlarge the electrical double-layer and create a proper condition for separating the crude oil acidic components from the rock's surface. Meanwhile,  $\text{SO}_4^{2-}$  ion can decrease the rock surface's positive charge and boost the process of wettability alteration by  $\text{Mg}^{2+}$  and  $\text{Ca}^{2+}$  ions (Fathi et al. 2010a, b).

Aside from imbibing brine salinity, some research focuses on the impact of connate brine salinity on oil recovery. Mechanisms of the effect of the connate brine on the oil recovery are analogous to that of imbibing brine (i.e., lowering the salinity). Moreover, the PDIs participation in the connate brine has a positive effect on the oil recovery in the modified salinity brine imbibition (Mohammadkhani et al. 2018; Sharma and Filoco 2000; Shehata and Nasr-El-Din 2017).

It is shown that PDIs behave the same in chalk rocks as in limestone rocks, with the difference being that the reactivity in chalks is higher than in limestones (Shariatpanahi et al. 2010). Moreover, investigations have shown that the abovementioned chemical reactions for wettability alteration by modified salinity brine in dolomite rocks

**Table 1** Comparison of tests conditions scaled by Mattax and Kyte's, Ma et al.'s, Mason et al.'s and Bassir et al.'s scaling equations and the gathered tests in this study

Authors (Year)	Tests source	Number of tests	Lithology	Boundary condition	Imbibing brine salinity (ppm*)	Connate brine		$\frac{k_{ro}}{k_w}$	Test temperature (°C)	Aging
						Saturation (%)	Salinity (ppm)			
Mattax and Kyte (1962)	Mattax and Kyte (1962)	4	Alundum	OEO	0	0	–	9–9.4	Room temperature	No
		2	Sandstone	AFO				176		
Ma et al. (1997)	Mattax and Kyte (1962)	4	Alundum	OEO	0	0	–	9–9.4	Room temperature	No
		2	Sandstone	AFO				176		
	Hamon and Vidal (1986)	1	Aluminum silicate	AFO	0	13.2	0	11.5	20	No
		3		TEO		13.6–18.9				
		4		OEO		16.4–19.8				
	Zhang et al. (1996)	6	Sandstone	AFO	22,200	0	–	39	Room temperature	No
		1		TEO						
		3		TEC				4–162		
		3		OEO						
Mason et al. (2010)	Fischer and Morrow (2006)	27	Sandstone	AFO	35,587	0	–	0.01–43	20	No
	Fischer et al. (2008)	10		OEO	39,587			0.008–63		
		12		TEC				0.008–173		
Bassir et al. (2023)	14 references from 2010 to 2020	59	Limestone	AFO	438–97,225	9.1–68	43,800–292,200	3.5–43.8	60–130	Yes
This work	Ten references from 2006 to 2014	85	Chalk	AFO	10,010–54,380	8–54.6	41,823–82,100	1.81–10.90	50–130	Yes
	Three references from 2012 to 2020	12	Dolomite	AFO	3,340–66,625	16.9–40.1	189,412–222,190	4.6–9.6	70–90	
	Four references from 2016 to 2020	13	Sandstone	AFO	966–5,000	39.3–46.8	14,178–174,156	2.6–15.2	50–90	

\*Parts per million

are not different from the other carbonates (Shariatpanahi et al. 2016).

Oil recovery improvement mechanisms in sandstones are similar to those of carbonates but have differences. Contrary to carbonates, anionic groups of crude oil's organic acid (e.g., carboxylate) adsorb on the sandstones' mineral surfaces with a negative charge via calcium bridges instead of sodium bridges or van der Waals forces. Consequently, decreasing salinity can enhance the electrostatic repulsive forces between carboxylate groups and mineral surfaces and unravel calcium bridges to make the rock surface wettability more water-wet (Yang et al. 2016). Moreover, investigations have demonstrated that reservoir sandstone cores saturated by connate brine comprising divalent cations ( $\text{Ca}^{2+}$  and  $\text{Mg}^{2+}$ ) show more oil recovery than the cores saturated by monovalent cations ( $\text{Na}^+$ ) (Shehata and Nasr-El-Din 2017).

Some other mechanisms are suggested, such as microdispersion formation and mineral dissolution, but they are not widely accepted as the principal mechanism of improving oil recovery by modified salinity brine imbibition (Mahani et al. 2015; Mahzari et al. 2019). Consequently, the multi-ion exchange is generally believed to be the critical mechanism of the oil recovery enhancement during modified salinity brine imbibition, as is considered in our investigations.

### Literature analysis and novelties of this work

From Table 1, the following limitations in the literature scaling equations can be shown. This research tries to resolve these limitations.

1. No scaling equation includes the effect of the imbibition of a modified salinity imbibing brine into a chalk/dolomite/sandstone rock containing higher salinity connate brine. Our recent work proposes a new scaling equation for such conditions only in limestones (Bassir et al. 2023).
2. All literature scaling equations are justified by spontaneous imbibition experiments at room temperature and no initial aging conditions toward an oil-wet state (far from reservoir conditions).
3. Due to the specific properties of each lithology, such as tortuosity, mineral type and grain packing and sorting, scaling equations should be defined separately for each lithology.
4. The properties of the connate brine are not included explicitly in the literature scaling equations. Mixing of imbibing and connate brines may cause memorable interactions that must be checked.
5. Most of the developed scaling equations in the literature are for a water-wet situation and an unchanged wettability during the test. During modified salinity brine injection, it is generally accepted that a wettability altera-

tion to a more water-wet state occurs and is crucial. The duration of all the collected experiments in this study is extended sufficiently until no oil is produced from the core samples. Consequently, the wettability alteration becomes complete as the leading cause of improved recovery.

## Data and methods

### Data acquisition

In this section, all the 110 literature spontaneous imbibition experimental data that are collected and used in our study are discussed. This research will consider spontaneous imbibition experimental tests with a boundary condition of AFO representing a cylindrical core (matrix block) immersed in the imbibing brine. The data analysis shows that some required parameters are not reported in the corresponding references. The viscosity of crude oil and brine and the IFT between crude oil and imbibing brine are among those nonreported data. Therefore, these parameters are produced. For this purpose, the most accepted correlations in literature defined based on experimental data (Abooali et al. 2019; Glaso 1980; Numbere et al. 1977) with an acceptable error range are used. These correlations (Abooali et al.'s correlation for IFT, Glaso's correlation for oil viscosity and Numbere et al.'s correlation for brine viscosity) are explained in detail in Appendix A.

To select proper correlations for computing the non-reported properties, operative ranges of the published correlations were compared to the gathered data. The correlations with a good matching to the collected data properties were chosen. This comparison is shown in Table 7 (Appendix A). Some other critical non-reported data, such as crude oil total acid number (TAN) and core dimensions, cannot be estimated. This data is achieved by communication with the papers' authors. A plot digitizer software digitizes the published oil recovery curves to find the exact oil recovery data values (i.e., time and oil recovery percent (%IOIP)).

For chalks, 85 experimental data from ten references published between 2006 and 2014 are gathered (Fathi et al. 2010a, b; Fathi et al. 2011a, 2011b; Fathi et al. 2010a, b; Kazankapov 2014; Puntervold et al. 2009; Strand et al. 2008; Zhang and Austad 2006; Zhang et al. 2006, 2007). For dolomites, 12 test data from three references published between 2012 and 2020 are collected (Mehraban et al. 2020; Romanuka et al. 2012; Shariatpanahi et al. 2016). For sandstones, 13 experimental data from four references published between 2016 and 2020 are gathered (Al-Saedi et al. 2020, 2019; Shehata and Nasr-El-Din 2017; Yang et al. 2016). In these experiments, a modified salinity brine is imbibed

spontaneously into an oil-saturated rock sample containing a higher salinity connate brine.

In Table 2, all the data used to find new scaling equations for chalk, dolomite and sandstone samples are shown, respectively.  $I_w$  and  $I_{wi}$  denote imbibing and connate brines ionic strengths, respectively (this data is shown in Sect. "Methods").

Some of the literature experimental data not included explicitly in the new scaling equations are shown in Table 3. This table show the range of the data to which new scaling equations apply. All these parameters are reported directly in the references. Details are shown in Appendix B. It is remarkable that in the articles in which the TAN is not mentioned, the IFT value is noted instead. This data can clarify the range of the applicability of our newly proposed scaling equations. Moreover, the effect of these parameters is applied to the new scaling equations; for example, temperature and °API affect viscosities and the brines salinities are reflected in their viscosities and ionic strengths. The five reported ions (Sodium, Chlorine, Magnesium, Calcium and Sulfate) include the brine's bulk of salts. The concentration of other ions (such as potassium, strontium, barium, bicarbonate, etc.,) is less than 1% of the total salinity of each brine and, therefore, can be neglected because very few studies report the significant effect of these minor ions on the oil recovery improvement process by modified salinity brine in the literature.

In all experiments, the rock samples' initial wettability can be considered oil-/mixed-wet due to the aging process before the tests start. Because the vital mechanism of the modified salinity brine effect for recovery improvement is believed to be wettability alteration, the wettability of all the rock samples assumed to be changed to a less oil-wet state during the tests (Fathi et al. 2010a, b, 2011a, 2010a; Puntervold et al. 2007, 2009; Shariatpanahi et al. 2016).

All the collected literature experiments are performed at atmospheric pressure; hence, the crude oils are all "dead oil" which is the weak point of the data far from the reservoir conditions with typically live oil. Our investigations show no spontaneous imbibition tests in the literature used modified salinity brine and live oil. This topic must be addressed in the future in this research area, both in experimental and scaling studies.

## Methods

In the first stage of this research, Mattax and Kyte's, Ma et al.'s and Mason et al.'s scaling equations (as shown in Sect. "Scaling equations") are used to scale the literature experimental data of spontaneous imbibition by modified salinity brine in three lithologies rock samples (i.e., chalk, dolomite and sandstone). This analysis shows the scaling strength of each equation and chooses the equation with

the lowest error that can be used as the base equation for developing a new scaling equation for each lithology.

As shown in Tables 8, 9, 10 (Appendix B), each of the collected tests has a specific  $R_\infty$  and  $t_{\text{end}}$ . Hence, the oil recovery at each time step is normalized relative to its  $R_\infty$ ; by this method, the normalized oil recovery of each experiment varies between zero and one. The normalized recovery data are plotted versus a horizontal semi-log plot axis of dimensionless time. For each lithology, all scaled recovery data by the three scaling equations are drawn on similar log cycles for a fair comparison among the scaling quality of different equations. Moreover, the arithmetic mean of the data scatter is used to better compare the scaling accuracy of the scaling equations. The data scatter at specific y-axis values (i.e., 0, 0.1, 0.2, 0.3, 0.4, 0.5, 0.6, 0.7, 0.8, 0.9 and 1) are determined and averaged arithmetically to calculate this mean value.

According to the mechanisms described in Sect. "Mechanisms of oil recovery improvement by modified salinity imbibing brine" and the methodology explained in our recent work (Bassir et al. 2023), both imbibing and connate brines ionic strengths ( $I_w$  and  $I_{wi}$ , respectively) are used to develop a new scaling equation for the scaling of spontaneous imbibition by modified salinity imbibing brine in limestone rocks. Here, we repeat the same method for the literature experimental data on chinks, dolomites, and sandstones. After that, the data of all four lithologies is used to develop a general scaling equation that can be applied regardless of lithology.

The ionic strength ( $I$ ) concept is introduced by Hückel and Debye (1923):

$$I = \frac{1}{2} \sum_{i=1}^n c_i z_i^2, \quad (6)$$

where  $z$  and  $c$  are each ion's charge number and molar concentration (mol/L), respectively (Hückel and Debye 1923). Based on Eq. (6), due to the charge number exponent, the impact of the divalent ions (such as  $\text{Mg}^{2+}$  and  $\text{SO}_4^{2-}$ ) is four times that of monovalent ions (such as  $\text{Na}^+$  and  $\text{Cl}^-$ ). The ionic strength has the advantage of independence from the temperature. We applied their ionic strengths to make a dimensionless parameter to add to the base scaling equations for considering the impact of both imbibing and connate brines' PDIs. The ratio of imbibing to connate brines ionic strengths ( $\frac{I_w}{I_{wi}}$ ) is the simplest dimensionless form that can be assumed. If the imbibing and connate brines have a similar ionic composition, the effect of this ratio will be eliminated (becomes one).

Literature studies (Bassir et al. 2023) show that the oil recovery and  $\frac{I_w}{I_{wi}}$  term do not have a distinctive direct/inverse relationship. An empirical exponent is allocated to

**Table 2** Principal properties of the gathered tests performed on chalk, dolomite and sandstone samples

Author(s) (Year)	Rock				Crude oil	Crude oil/ imbibing brine	Imbibing brine		Connate brine	
	$k$ (mD)	$\phi$ (Fraction)	$L$ (cm)	$D$ (cm)	$\mu_o^*$ (cp)	$\sigma^{**}$ (mN/m)	$\mu_w^{***}$ (cp)	$I_w$ (mol/L)	$I_{wi}$ (mol/L)	
<b>Chalk</b>										
Zhang and Austad (2006)	3.5	0.49	6.40	3.55	0.85	33.1	0.431	0.657	1.452	
	3.5	0.49	5.80	3.51	0.85	33.1	0.432	0.657	1.452	
	3.5	0.49	6.05	3.53	0.85	33.1	0.432	0.657	1.452	
	3.5	0.47	5.96	3.54	0.63	34.8	0.303	0.657	1.452	
	3.5	0.49	5.91	3.54	0.63	34.8	0.302	0.657	1.452	
	3.5	0.49	5.70	3.54	0.63	34.8	0.302	0.657	1.452	
	3.5	0.49	5.77	3.54	0.63	34.8	0.302	0.657	1.452	
	3.5	0.49	5.52	3.54	0.63	34.8	0.301	0.657	1.452	
	3.5	0.50	4.83	3.54	0.63	34.8	0.304	0.657	1.452	
	3.5	0.49	5.93	3.48	0.47	33.4	0.230	0.657	1.452	
	3.5	0.48	5.95	3.48	0.47	33.4	0.231	0.657	1.452	
	3.5	0.48	5.98	3.48	0.47	33.4	0.230	0.657	1.452	
	3.5	0.49	4.87	3.48	0.47	33.4	0.230	0.657	1.452	
	Zhang et al. (2006)	3.5	0.48	5.85	3.51	0.63	34.8	0.301	0.657	1.015
		3.5	0.49	5.58	3.54	0.89	36.3	0.431	0.657	1.452
3.5		0.49	5.58	3.54	0.63	34.8	0.303	0.657	1.068	
3.5		0.49	6.33	3.51	0.89	36.3	0.432	0.657	1.452	
3.5		0.48	5.45	3.55	0.63	34.8	0.301	0.657	1.452	
3.5		0.48	5.45	3.55	0.47	33.4	0.229	0.657	1.119	
3.5		0.49	5.32	3.55	0.63	34.8	0.303	0.657	1.452	
3.5		0.49	5.32	3.55	0.47	33.4	0.231	0.657	1.137	
3.5		0.48	4.85	3.55	0.63	34.8	0.303	0.657	1.452	
3.5		0.48	4.85	3.55	0.47	33.4	0.231	0.657	1.161	
3.5		0.48	6.08	3.54	0.47	33.4	0.231	0.657	1.452	
3.5		0.47	6.41	3.54	0.47	33.4	0.229	0.657	1.452	
3.5		0.47	5.93	3.54	0.47	33.4	0.231	0.657	1.452	
3.5		0.49	6.55	3.52	0.85	33.1	0.431	0.657	1.452	
3.5		0.50	5.94	3.44	0.85	33.1	0.431	0.657	1.452	
3.5	0.49	6.39	3.55	0.85	33.1	0.431	0.657	1.452		
3.5	0.50	6.06	3.52	0.85	33.1	0.432	0.657	1.452		
3.5	0.49	5.78	3.51	0.85	33.1	0.432	0.657	1.452		
Zhang et al. (2007)	3.5	0.47	6.23	3.57	0.63	34.8	0.306	0.741	1.218	
	3.5	0.47	6.23	3.57	0.47	33.4	0.233	0.741	1.086	
	3.5	0.49	5.90	3.57	0.63	34.8	0.307	0.741	1.221	
	3.5	0.49	5.90	3.57	0.47	33.4	0.234	0.741	1.149	
	3.5	0.48	6.15	3.57	0.63	34.8	0.305	0.677	1.207	
	3.5	0.48	6.15	3.57	0.47	33.4	0.233	0.677	1.091	
	3.5	0.49	6.25	3.57	0.63	34.8	0.305	0.741	1.201	
	3.5	0.49	6.25	3.57	0.47	33.4	0.232	0.741	1.032	
	3.5	0.47	5.80	3.50	0.85	33.1	0.433	0.657	1.024	
	3.5	0.47	5.84	3.50	0.85	33.1	0.432	0.657	1.240	
3.5	0.49	5.25	3.50	0.89	36.3	0.434	0.657	1.322		
3.5	0.49	5.25	3.50	0.89	36.3	0.433	0.657	1.258		



**Table 2** (continued)

Author(s) (Year)	Rock				Crude oil	Crude oil/ imbibing brine	Imbibing brine		Connate brine
	$k$ (mD)	$\phi$ (Fraction)	$L$ (cm)	$D$ (cm)	$\mu_o^*$ (cp)	$\sigma^{**}$ (mN/m)	$\mu_w^{***}$ (cp)	$I_w$ (mol/L)	$I_{wi}$ (mol/L)
	3.5	0.49	5.25	3.50	0.63	34.8	0.304	0.657	1.235
	3.5	0.49	5.25	3.50	0.47	33.4	0.232	0.657	1.153
	3.5	0.49	6.45	3.50	0.89	36.3	0.434	0.657	1.292
	3.5	0.49	6.45	3.50	0.63	34.8	0.304	0.657	1.252
	3.5	0.49	6.45	3.50	0.47	33.4	0.231	0.657	1.154
Strand et al. (2008)	1.5	0.48	6.50	3.80	0.47	33.3	0.251	0.660	0.869
Puntervold et al. (2009)	1.5	0.49	6.50	3.80	1.13	34.4	0.606	0.985	1.112
	1.5	0.48	6.50	3.80	1.13	34.4	0.600	0.904	1.112
	1.5	0.49	6.50	3.80	1.13	34.4	0.586	0.711	1.112
	1.5	0.46	6.50	3.80	0.83	33.2	0.435	0.711	1.112
	1.5	0.50	6.50	3.80	0.83	33.2	0.445	0.904	1.112
	1.5	0.49	6.50	3.80	0.83	33.2	0.435	0.711	1.112
	1.5	0.47	6.50	3.80	0.65	32.0	0.353	0.985	1.112
	1.5	0.46	6.50	3.80	0.65	32.0	0.349	0.904	1.112
	1.5	0.48	6.50	3.80	0.65	32.0	0.340	0.711	1.112
	1.5	0.47	6.50	3.80	0.53	30.8	0.284	0.904	1.112
	1.5	0.45	6.50	3.80	0.53	30.8	0.281	0.821	1.112
	1.5	0.47	6.50	3.80	0.53	30.8	0.277	0.711	1.112
	1.5	0.47	6.50	3.80	0.45	30.1	0.239	0.904	1.112
	1.5	0.49	6.50	3.80	0.45	30.1	0.233	0.711	1.112
Fathi et al. (2010a)	1.5	0.45	7.00	3.81	0.68	33.7	0.303	0.657	1.112
	1.5	0.46	7.00	3.81	0.62	33.2	0.275	0.657	1.112
	1.5	0.45	7.00	3.81	0.56	32.7	0.237	0.257	1.112
	1.5	0.45	6.92	3.81	0.56	32.7	0.251	0.657	1.112
Fathi et al. (2010b)	3.5	0.46	6.93	3.81	0.62	32.7	0.275	0.657	0.832
	3.5	0.46	6.99	3.81	0.62	32.7	0.275	0.657	0.809
	3.5	0.45	7.10	3.80	0.64	31.5	0.275	0.657	0.790
	3.5	0.44	6.97	3.81	0.64	31.5	0.275	0.657	0.792
Fathi et al. (2011a)	2	0.45	7.02	3.81	0.60	33.3	0.275	0.657	0.866
	2	0.45	7.06	3.80	0.60	33.3	0.275	0.657	0.854
	2	0.44	7.02	3.81	0.59	33.4	0.275	0.657	0.827
	2	0.45	7.02	3.81	0.59	33.4	0.275	0.657	0.826
Fathi et al. (2011b)	1.5	0.46	7.00	3.80	0.78	33.5	0.417	0.473	1.112
	1.5	0.44	7.00	3.80	0.78	33.5	0.411	0.257	1.112
	1.5	0.47	7.00	3.80	0.61	32.2	0.325	0.473	1.112
	1.5	0.46	7.00	3.80	0.61	32.2	0.337	0.657	1.112
	1.5	0.48	7.00	3.80	0.73	33.8	0.288	0.368	1.112
	1.5	0.46	7.00	3.80	0.73	33.8	0.287	0.257	1.112
	1.5	0.48	7.00	3.80	0.59	32.9	0.241	0.473	1.112
Kazankapov (2014)	1.5	0.46	7.02	3.79	3.49	27.5	0.320	0.257	1.112
	1.5	0.47	7.02	3.80	3.49	27.5	0.325	0.473	1.112
	1.5	0.46	7.02	3.80	3.49	27.5	0.337	0.657	1.112
Minimum	<b>1.5</b>	<b>0.44</b>	<b>4.83</b>	<b>3.44</b>	<b>0.45</b>	<b>27.5</b>	<b>0.229</b>	<b>0.257</b>	<b>0.790</b>
Arithmetic mean	<b>2.7</b>	<b>0.48</b>	<b>6.25</b>	<b>3.65</b>	<b>0.76</b>	<b>33.3</b>	<b>0.325</b>	<b>0.661</b>	<b>1.200</b>
Maximum	<b>3.5</b>	<b>0.50</b>	<b>7.10</b>	<b>3.81</b>	<b>3.49</b>	<b>36.3</b>	<b>0.606</b>	<b>0.985</b>	<b>1.452</b>

**Table 2** (continued)

Author(s) (Year)	Rock				Crude oil	Crude oil/ imbibing brine	Imbibing brine		Connate brine
	$k$ (mD)	$\phi$ (Fraction)	$L$ (cm)	$D$ (cm)	$\mu_o^*$ (cp)	$\sigma^{**}$ (mN/m)	$\mu_w^{***}$ (cp)	$I_w$ (mol/L)	$I_{wi}$ (mol/L)
<b>Dolomite</b>									
Romanuka et al. (2012)	201.0	0.19	5.00 <sup>+</sup>	3.81 <sup>+</sup>	3.9	22.7	0.431	0.660	4.351
	201.0	0.19	5.00 <sup>+</sup>	3.81 <sup>+</sup>	3.9	22.7	0.404	0.070	4.049
	235.0	0.20	5.00 <sup>+</sup>	3.81 <sup>+</sup>	3.9	22.7	0.431	0.660	4.351
	235.0	0.20	5.00 <sup>+</sup>	3.81 <sup>+</sup>	3.9	22.7	0.404	0.070	4.127
Shariatpanahi et al. (2016)	201.0	0.19	4.97	3.77	2.0	27.8	0.432	0.657	4.379
	201.0	0.19	4.97	3.77	2.0	27.8	0.404	0.066	4.202
	235.0	0.20	4.95	3.77	2.0	27.8	0.432	0.657	4.379
	235.0	0.20	4.95	3.77	2.0	27.8	0.404	0.066	4.115
Mehraban et al. (2020)	35.4	0.18	7.13	3.82	2.3	23.4	0.355	0.860	3.659
	34.2	0.19	7.54	3.82	2.3	23.4	0.357	0.917	3.659
	27.7	0.18	7.44	3.82	2.3	23.4	0.348	0.833	3.659
	38.4	0.19	7.62	3.82	2.3	23.4	0.362	1.049	3.659
Minimum	<b>27.7</b>	<b>0.18</b>	<b>4.95</b>	<b>3.77</b>	<b>2.0</b>	<b>22.7</b>	<b>0.348</b>	<b>0.066</b>	<b>3.659</b>
Arithmetic mean	<b>156.6</b>	<b>0.19</b>	<b>5.80</b>	<b>3.80</b>	<b>2.7</b>	<b>24.6</b>	<b>0.397</b>	<b>0.547</b>	<b>4.049</b>
Maximum	<b>235.0</b>	<b>0.20</b>	<b>7.62</b>	<b>3.82</b>	<b>3.9</b>	<b>27.8</b>	<b>0.432</b>	<b>1.049</b>	<b>4.379</b>
<b>Sandstone</b>									
Yang et al. (2016)	82.5	0.21	7.01	3.81	2.0	34.7	0.465	0.027	0.676
	92.7	0.22	6.99	3.80	2.0	34.7	0.465	0.027	0.383
Shehata and Nasr-El-Din (2017)	164.0	0.18	50.80	3.81	6.5	31.0	0.430	0.086	3.361
Al-Saedi et al. (2019)	95.0	0.21	14.90	2.54	0.8*	31.0	0.313	0.017	1.750
	95.0	0.21	14.87	2.54	0.8*	31.0	0.313	0.017	1.750
	94.0	0.21	14.80	2.54	0.8*	31.0	0.313	0.017	1.750
	109.0	0.21	15.00	2.54	0.8*	31.0	0.313	0.017	1.750
Al-Saedi et al. (2020)	1.7	0.17	10.10	2.54	1.6*	34.0	0.547	0.021	2.047
	50.0	0.17	10.10	2.54	1.6*	34.0	0.547	0.021	2.047
	2.0	0.18	9.70	2.54	1.6*	32.7	0.547	0.021	2.047
	51.0	0.18	9.62	2.54	1.6*	32.7	0.547	0.021	2.047
	2.3	0.19	9.52	2.54	1.6*	32.8	0.547	0.021	2.047
	48.6	0.18	9.50	2.54	1.6*	32.8	0.547	0.021	2.047
	Minimum	<b>1.7</b>	<b>0.17</b>	<b>6.99</b>	<b>2.54</b>	<b>0.8</b>	<b>31.0</b>	<b>0.313</b>	<b>0.017</b>
Arithmetic mean	<b>68.3</b>	<b>0.19</b>	<b>14.07</b>	<b>2.83</b>	<b>1.8</b>	<b>32.6</b>	<b>0.453</b>	<b>0.025</b>	<b>1.823</b>
Maximum	<b>164.0</b>	<b>0.22</b>	<b>50.80</b>	<b>3.81</b>	<b>6.5</b>	<b>34.7</b>	<b>0.547</b>	<b>0.086</b>	<b>3.361</b>

Bold row(s) indicate a conclusion from the other rows

+ Achieved by communication with the papers' authors

\*Crude oil viscosities that are computed by Glaso's correlation (Glaso 1980)

\*\*All the oil/brine IFTs are estimated by Abooli et al.'s correlation (Abooli et al. 2019)

\*\*\*The viscosity of all the imbibing brines is calculated by Numbere et al.'s correlation (Numbere et al. 1977)

**Table 3** Range of the properties of the literature experimental data performed on chalk, dolomite and sandstone samples that are not included explicitly in the scaling equations

Lithology	Chalk			Dolomite			Sandstone		
	Minimum	Arithmetic mean	Maximum	Minimum	Arithmetic mean	Maximum	Minimum	Arithmetic mean	Maximum
Testis properties									
Test temperature (°C)	50	99	130	70	77	90	50	65	90
Aging temperature (°C)	90	90	90	70	82	90	60	85	90
Aging time (Days)	28	34	57	21	30	40	14	30	42
°API	28.2	43.6	45.8	30.0	32.3	35.6	39.4	41.9	45.2
TAN (mgKOH/g)	0.39	1.57	2.80	0.14	0.53	0.92	0.16	0.88	1.55
$\mu_v/\mu_w$	1.81	2.35	10.90	4.6	6.9	9.6	2.6	4.0	15.2
$\mu_{vt}$ (cp)	0.241	0.348	0.616	0.500	0.627	0.707	0.390	0.554	0.673
Imbibing brine salt concentration ( $C_{s,wb}$ ) (ppm)	10,010	33,441	54,380	3340	31,640	66,625	966	1348	5000
Connate brine salt concentration ( $C_{s,wt}$ ) (ppm)	41,823	65,174	82,100	189,412	206,524	222,190	14,178	95,433	174,156
$I_w/I_{wt}$	0.231	0.567	0.886	0.016	0.139	0.287	0.009	0.018	0.070
Total time of recovery ( $t_{end}$ ) (Days)	4	32	91	5	23	38	3.3	24.4	41.0
$R_{\infty}$ (Fraction of IOIP)	0.03	0.34	0.70	0.01	0.18	0.44	0.04	0.22	0.64
Imbibing brine ionic composition									
Sodium (ppm)	1150	10,634	19,182	27	4651	10,350	0	392	1967
Chlorine (ppm)	4467	18,229	32,085	1861	19,179	42,448	565	772	3033
Magnesium (ppm)	0	945	1094	109	4490	14,019	0	29	62
Calcium (ppm)	0	636	2084	0	356	660	0	61	361
Sulfate (ppm)	0	2762	9222	0	2613	12,105	0	28	62
Connate brine ionic composition									
Sodium (ppm)	11,324	22,502	30,797	56,993	61,296	65,527	0	29,411	54,400
Chlorine (ppm)	24,490	39,439	50,131	113,672	126,545	137,097	9058	57,821	107,000
Magnesium (ppm)	0	435	873	660	1677	2236	0	1094	4326
Calcium (ppm)	0	2174	9258	14,548	15,589	16,592	0	6059	10,600
Sulfate (ppm)	0	418	4542	179	730	1750	0	200	372

the  $\frac{I_w}{I_{wi}}$  ratio to finalize this complex issue. Based on this survey, the general form of the new scaling equations is:

$$t_{D-New} = (\text{The best literature scaling equation}) \left( \frac{I_w}{I_{wi}} \right)^N, \quad (7)$$

where  $N$  is the suggested empirical exponent.  $N$  can be positive or negative to demonstrate the direct/inverse relationship between the spontaneous imbibition oil recovery of the modified salinity brine and  $\frac{I_w}{I_{wi}}$  term for each lithology. To find the empirical exponents, a reasonable extensive arbitrary interval for  $N$  is tested and the final exponents for each lithology are selected by gradually narrowing the interval. This trial and error method examines negative to positive values. The empirical exponent with the lowest arithmetic mean of the data scatter is selected as the best one for each lithology.

Another point is that for a tall oil-wet block in a fractured reservoir that is immersed in imbibing brine, in addition to the capillary force, gravity force affects the oil recovery. In this study, we focus on the spontaneous imbibition oil recovery due to increased oil-imbibing brine capillary force as a result of wettability alteration to a more water-wet state caused by modified salinity brine and the oil recovery due to gravity force is neglected. The collected literature data in this study agrees with this assumption because the core samples' heights (as shown in Table 3) are short enough to ignore the effect of gravitational forces.

In general, scaling equations can be used to derive transfer functions that can be included in reservoir simulators. For this purpose, a mathematical expression with minimum matching parameters is needed. This study uses two models to fit the scaled data by our new scaling equations. The first model is similar to Aronofsky et al. model (Aronofsky et al. 1958) that links oil recovery and time with an exponential function as follows:

$$\frac{R}{R_\infty} = 1 - e^{-\lambda t_D}, \quad (8)$$

where  $\lambda$  is the constant of oil production decline applied as the matching parameter (Behbahani and Blunt 2005; Ma et al. 1997).

The second model suggested by Fries and Dreyer (2008) links oil recovery and time by applying Lambert's  $W$ -function (Abouzar Mirzaei-Paiaman 2015; Abouzar Mirzaei-Paiaman et al. 2011; Standnes 2010) as follows:

$$\frac{R}{R_\infty} = 1 + W(-e^{-1-at_D}) \quad (9)$$

where ' $a$ ' is a tuning parameter. Equation (10) can compute Lambert's  $W$ -function for  $-e^{-1} \leq x \leq 0$  with a maximum error of 0.1% (Fries and Dreyer 2008):

$$W(x) \approx -1 + \frac{\sqrt{2+2ex}}{1 + \frac{4.13501\sqrt{2+2ex}}{12.7036+\sqrt{2+2ex}}}, \quad (10)$$

where ' $x$ ' is any value between  $-e^{-1}$  and zero, and  $e$  is the Euler's number (2.71828). Using a trial and error technique and the root of mean square error (RMSE), these two models fitted to the scaled data of each lithology.

The stages of finding the matching parameters are similar to the arithmetic mean of the data scatter, with the difference that achieving the least value for the RMSE is favored here. RMSE can be calculated by:

$$\text{RMSE} = \sqrt{\frac{\sum_{i=1}^n (x_{\text{predicted}_i} - x_{\text{actual}_i})^2}{n}} \quad (11)$$

where  $x_{\text{actual}_i}$  and  $x_{\text{predicted}_i}$  are the actual and predicted values by model for each data point, respectively. Two mathematical expressions are developed based on the abovementioned models for each of the four new scaling equations (i.e., chalk, dolomite, sandstone and all lithology).

## Results and discussion

### Evaluation of the selected literature scaling equations

Figure 1a, b and c illustrate the scaling quality of Mattax and Kyte's, Ma et al.'s and Mason et al.'s scaling equations, respectively, to scale the literature 85 collected imbibition experimental data in chalk rock samples.

The same analysis is repeated for experimental recovery data for dolomite (12 tests) and sandstone (13 tests) rock samples, shown in Figs. 2 and 3, respectively.

As the recovery data becomes closer to each other, the scaling equation has more accuracy. However, as shown in Figs. 1, 2 and 3, the scaling quality of all the three scaling equations is poor and the scaling equations cannot converge recovery data points on a universal curve.

For each lithology, the arithmetic mean of data scatter is calculated and the scaling equation with the lowest arithmetic mean of data scatter is chosen for the next step of our study. Table 4 shows the process of comparing the scaling ability of various scaling equations for each lithology. Mattax and Kyte's scaling equation is chosen for chalk and dolomite rocks, and Mason et al.'s scaling equation is selected for sandstone rocks to be used for scaling equations development.

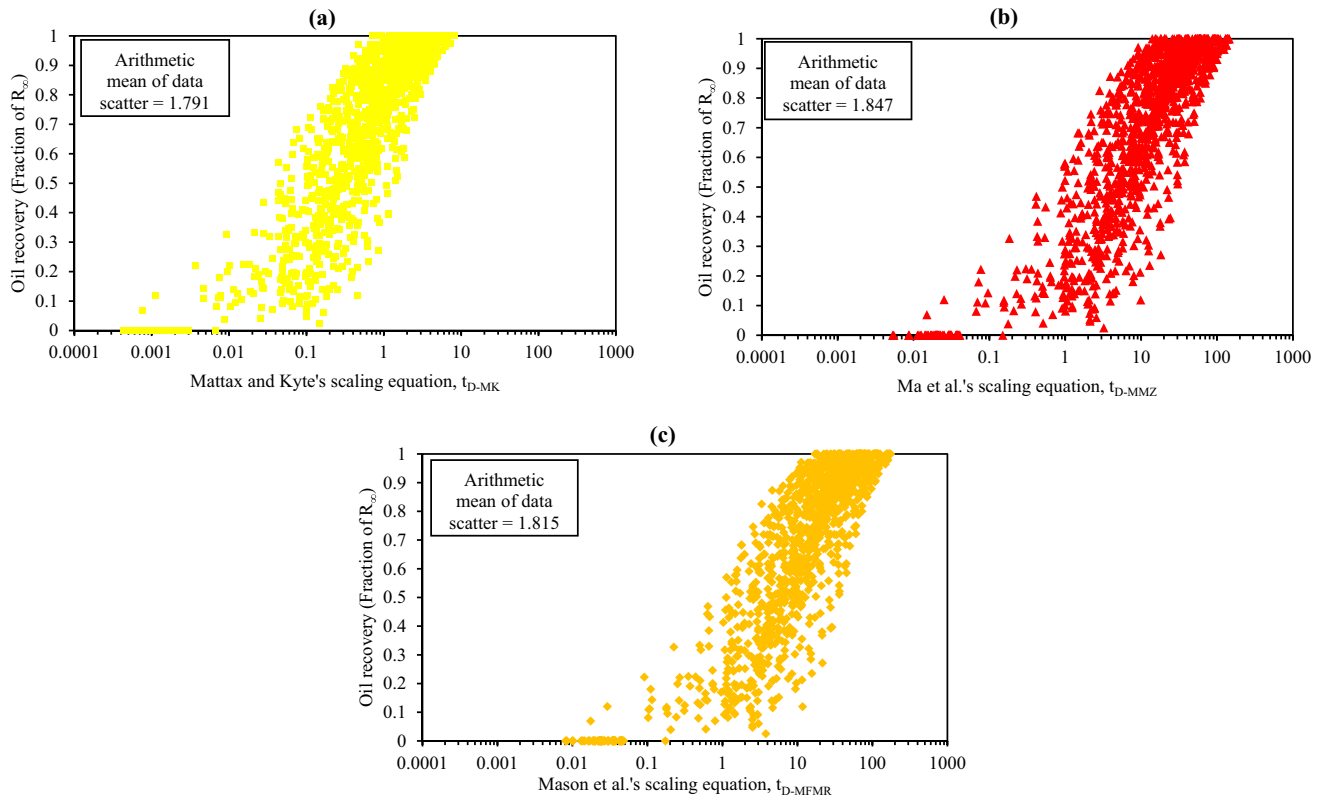


Fig. 1 Scaled recovery data by a Mattax and Kyte's, b Ma et al.'s and c Mason et al.'s scaling equations for 85 tests performed on chalk cores

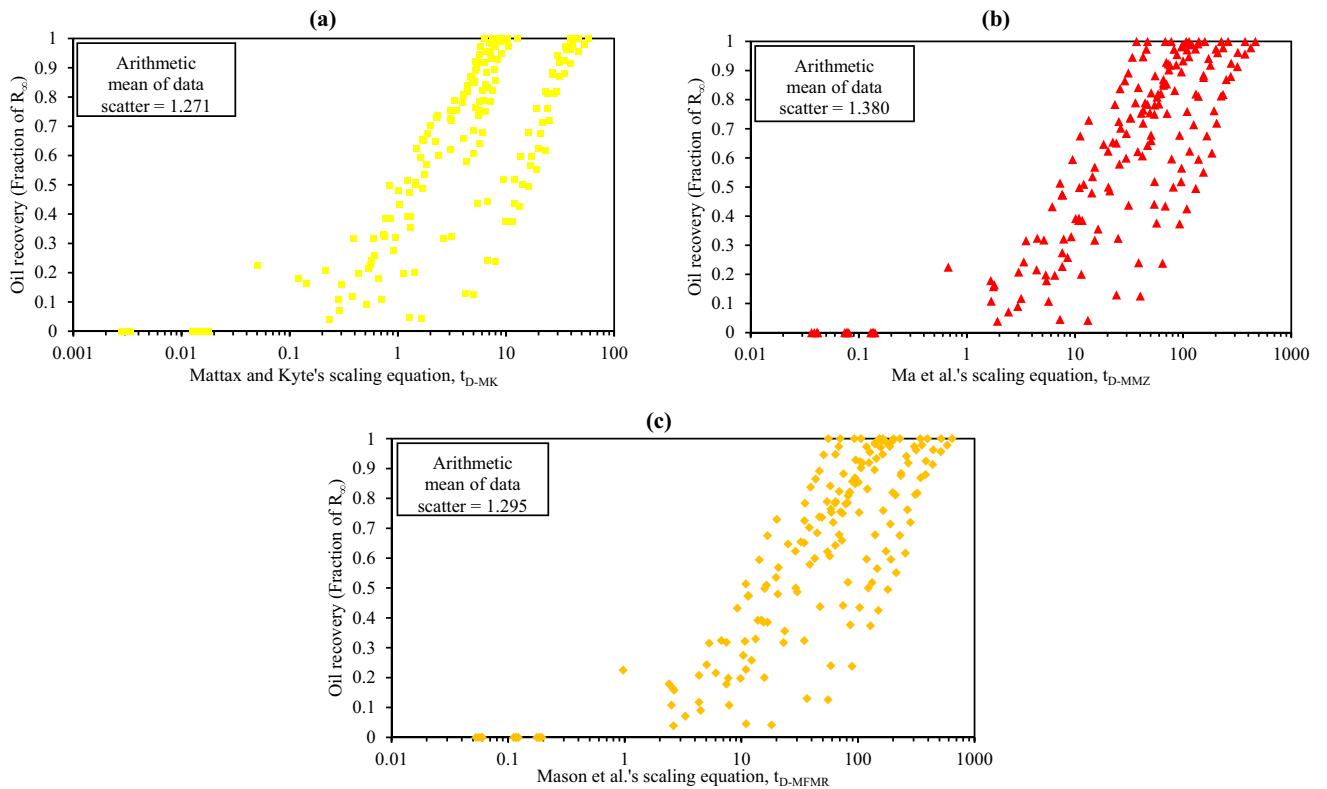
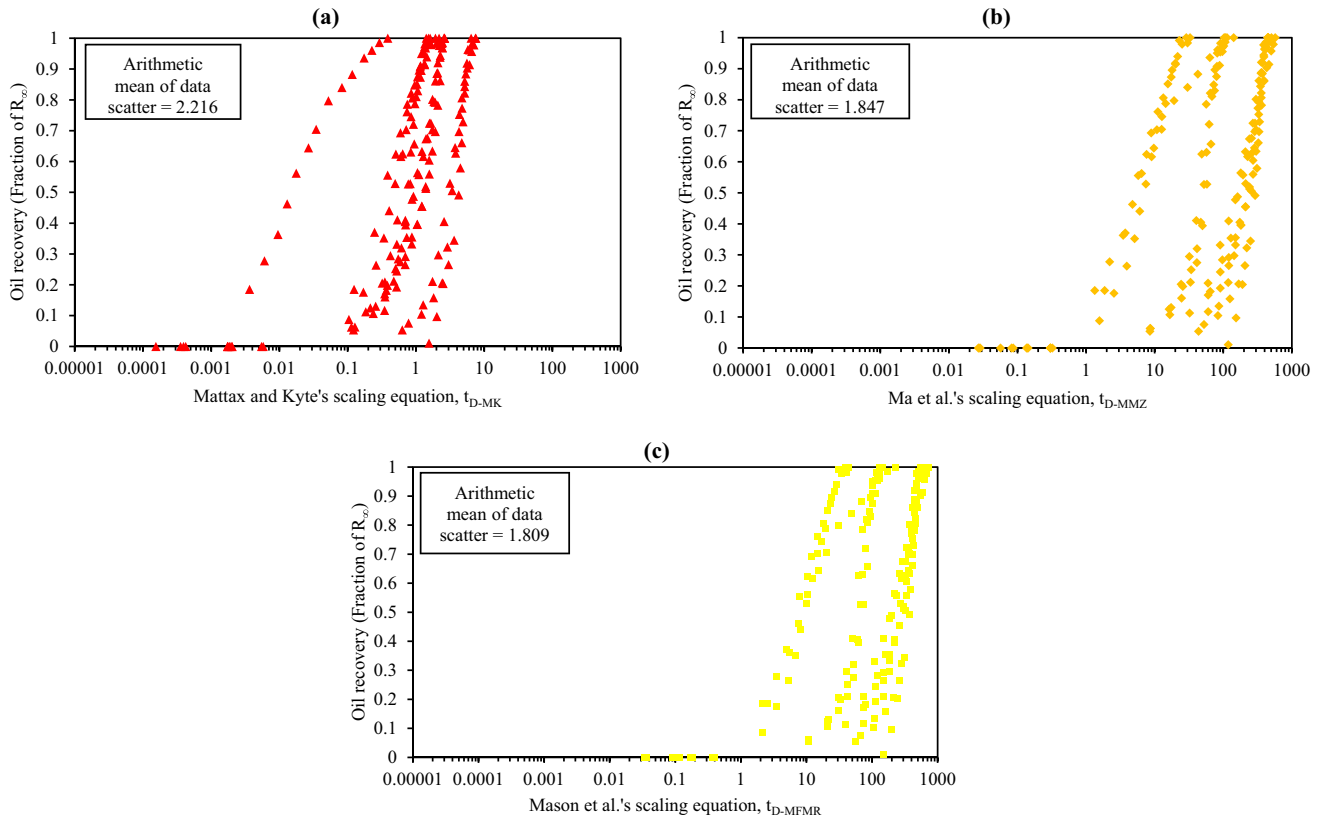


Fig. 2 Scaled recovery data by a Mattax and Kyte's, b Ma et al.'s and c Mason et al.'s scaling equations for 12 tests performed on dolomite cores



**Fig. 3** Scaled recovery data by **a** Mattax and Kyte's, **b** Ma et al.'s and **c** Mason et al.'s scaling equations for 13 tests performed on sandstone cores

**Table 4** The comparison of the arithmetic mean of data scatter of each scaling equation for different lithologies

	Mattax and Kyte	Ma et al.	Mason et al.	Selected scaling equation
Chalk	1.791	1.847	1.815	Mattax and Kyte
Dolomite	1.271	1.380	1.295	Mattax and Kyte
Sandstone	2.216	1.847	1.809	Mason et al.

**New scaling equations specific for each lithology**

Using Eq. (7) and the selected literature scaling equation for each lithology, the final form of the scaling equations for chalks, dolomites and sandstones, respectively, are as follows:

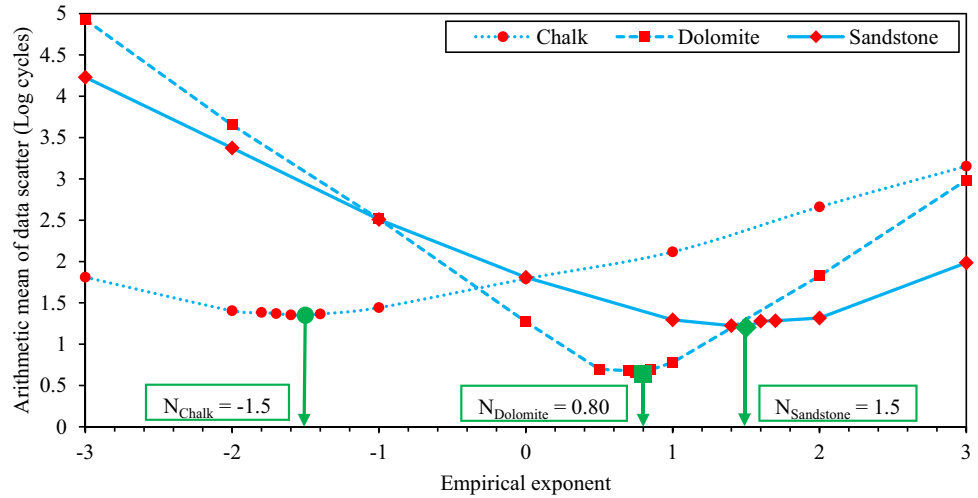
$$t_{D - Chalk} = t \sqrt{\frac{k}{\varphi} \frac{\sigma}{L^2} \frac{1}{\mu_w} \left( \frac{I_w}{I_{wi}} \right)^{N_{Chalk}}} \quad (12)$$

$$t_{D - Dolomite} = t \sqrt{\frac{k}{\varphi} \frac{\sigma}{L^2} \frac{1}{\mu_w} \left( \frac{I_w}{I_{wi}} \right)^{N_{Dolomite}}} \quad (13)$$

$$t_{D - Sandstone} = t \sqrt{\frac{k}{\varphi} \frac{\sigma}{L_c^2} \frac{2}{\mu_w + \sqrt{\mu_w \mu_o}} \left( \frac{I_w}{I_{wi}} \right)^{N_{Sandstone}}} \quad (14)$$

As shown in Fig. 4, for chalks, an exponent of (-1.5) with an arithmetic mean of data scatter of 1.349 log cycles, 24.7% less than Mattax and Kyte's scaling Eq. (1.791 log cycles), is achieved. For dolomites, an exponent of (+0.80) with an arithmetic mean of data scatter of 0.643 log cycles, 49.4% less than Mattax and Kyte's scaling Eq. (1.271 log cycles), is attained. An exponent of (+1.5) with an arithmetic mean of data scatter of 1.203 log cycles, 33.5% less than Mason et al.'s scaling Eq. (1.809 log cycles)] is achieved for sandstones. Because of the sharp increasing trend of the arithmetic mean of data scatter for the values below and above each gained empirical exponent, the acquired powers seem unique.

**Fig. 4** Optimization results for gaining the empirical exponent with the most minor arithmetic mean of data scatter for each lithology



Our new scaling equations for chalk, dolomite and sandstone lithologies are presented in Eqs. (15), (16) and (17), respectively.

$$t_{D - \text{Chalk}} = t \sqrt{\frac{k}{\phi} \frac{\sigma}{L^2} \frac{1}{\mu_w}} \left( \frac{I_w}{I_{wi}} \right)^{-1.5} \quad (15)$$

$$t_{D - \text{Dolomite}} = t \sqrt{\frac{k}{\phi} \frac{\sigma}{L^2} \frac{1}{\mu_w}} \left( \frac{I_w}{I_{wi}} \right)^{0.80} \quad (16)$$

$$t_{D - \text{Sandstone}} = t \sqrt{\frac{k}{\phi} \frac{\sigma}{L_c^2} \frac{2}{\mu_w + \sqrt{\mu_w \mu_o}}} \left( \frac{I_w}{I_{wi}} \right)^{1.5} \quad (17)$$

The negative value of N for chalk’s empirical exponent shows an inverse relationship between the  $\frac{I_w}{I_{wi}}$  term and spontaneous imbibition oil recovery in chalks, whereas in dolomites and sandstones, this relationship is direct because their empirical exponents are positive values. The different exponent sign of chalk compared to the other lithologies may be due to its unique porosity–permeability relationship. As shown in Table 2, the porosity ranges of chalk, dolomite and sandstone are 0.44–0.50, 0.18–0.20 and 0.17–0.22, respectively, whereas their permeability ranges are 1.5–3.5, 27.7–235 and 1.7–164 mD, respectively. These data show an unusual relationship between porosity and absolute permeability in chalks. Due to the vuggy structure of chalk rocks, their porosity is very high whereas their permeability is unexpectedly very low. This discrepancy might explain the different behavior of chalk compared to the other lithologies. More investigations are needed to clarify this disparity precisely.

The scaled data using the proposed scaling equations for each lithology is shown in Fig. 5.

### Matching data

The best fitted models to the scaled tests data for each lithology using corresponding scaling equations ( $t_D$ ) into Eqs. (8) and (9) are as follows:

$$\frac{R}{R_\infty} = 1 - e^{-0.93t_{D - \text{Chalk}}}; \text{RMSE} = 0.129 \quad (18)$$

$$\frac{R}{R_\infty} = 1 + W(-e^{-1-0.34t_{D - \text{Chalk}}}); \text{RMSE} = 0.111 \quad (19)$$

$$\frac{R}{R_\infty} = 1 - e^{-1.6t_{D - \text{Dolomite}}}; \text{RMSE} = 0.086 \quad (20)$$

$$\frac{R}{R_\infty} = 1 + W(-e^{-1-0.60t_{D - \text{Dolomite}}}); \text{RMSE} = 0.101 \quad (21)$$

$$\frac{R}{R_\infty} = 1 - e^{-5.3t_{D - \text{Sandstone}}}; \text{RMSE} = 0.238 \quad (22)$$

$$\frac{R}{R_\infty} = 1 + W(-e^{-1-1.9t_{D - \text{Sandstone}}}); \text{RMSE} = 0.221 \quad (23)$$

For chalks and sandstones, the Fries and Dreyer model and for dolomites, the Aronofsky et al. model have a better fit, as shown in Fig. 6. Equations (19), (20) and (23) can be used to develop a transfer function for the simulation of improved oil recovery by modified salinity brine in fractured chalk, dolomite and sandstone reservoirs, respectively (Abouzar Mirzaei-Paiaman et al. 2011; Tavassoli et al. 2005a, b).

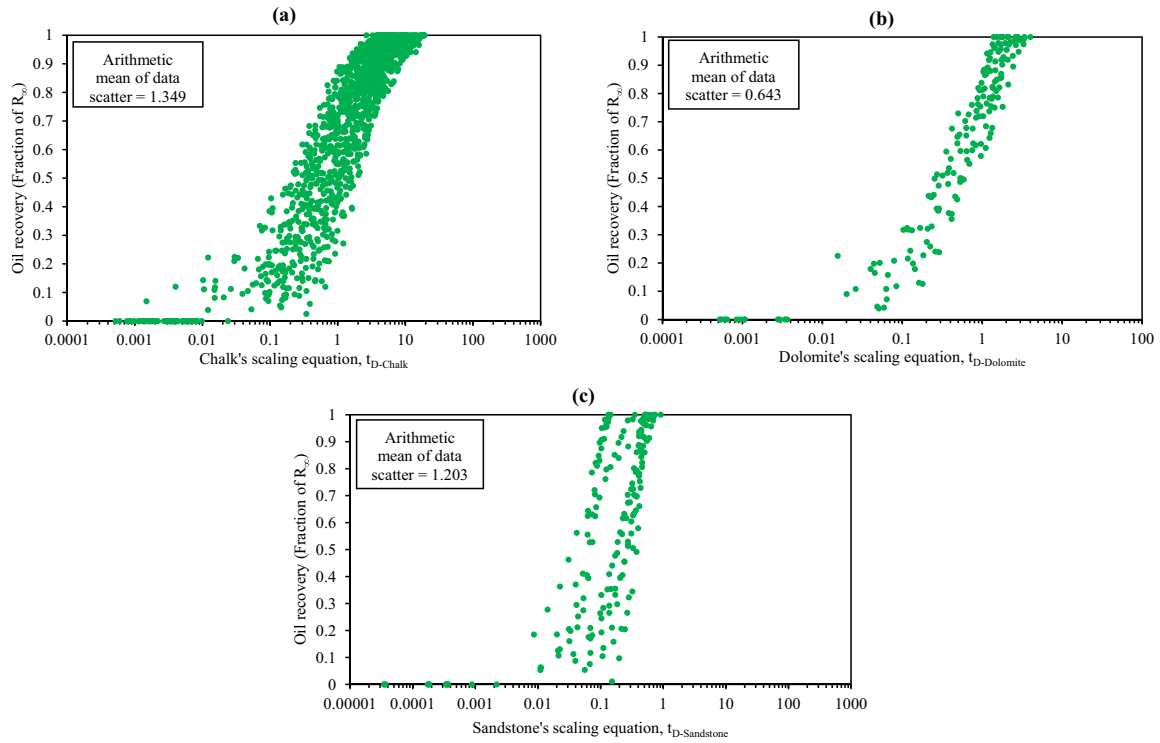


**Fig. 5** Scaled oil recovery data for **a** chalk, **b** dolomite and **c** sandstone tests by our newly proposed scaling equations

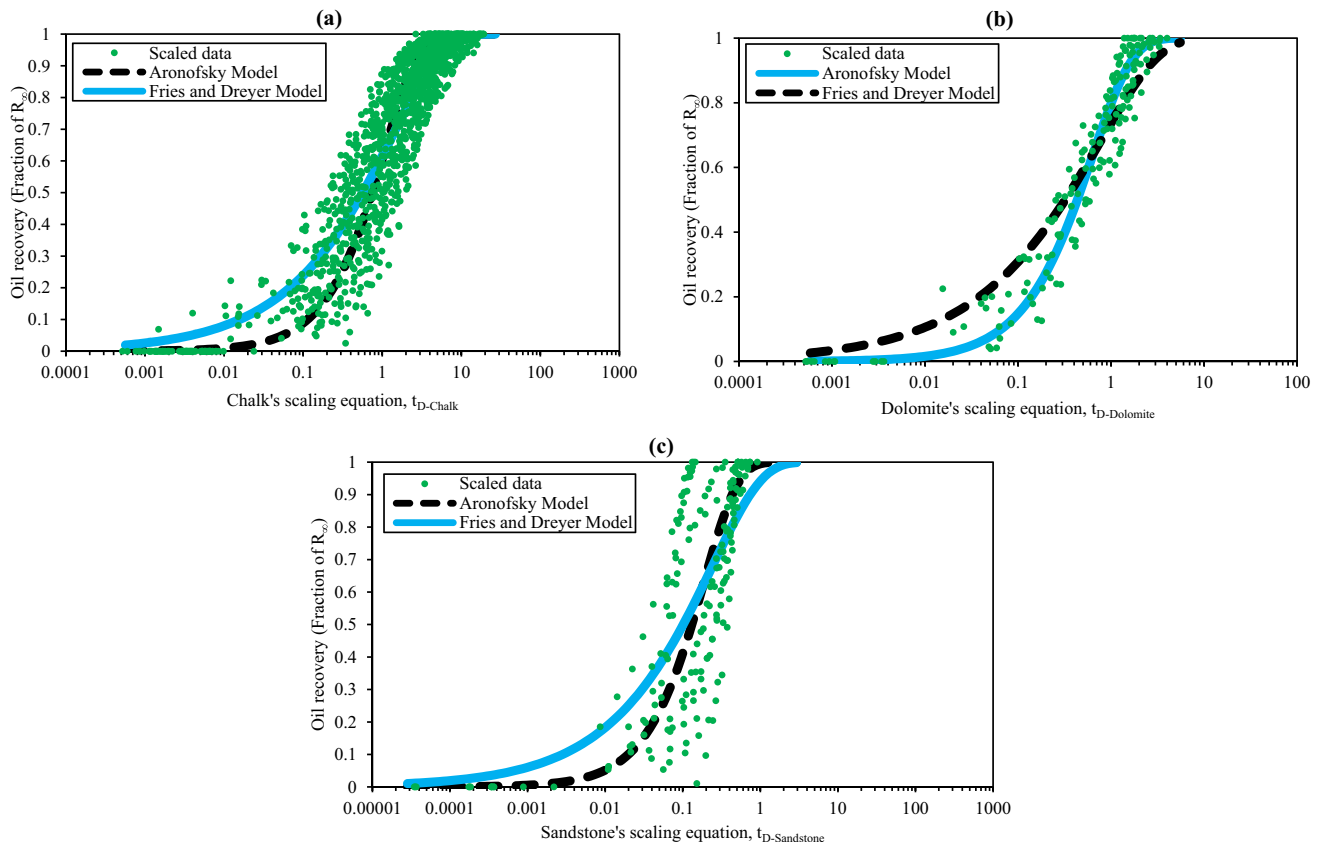


**Fig. 6** Best fitted models to the scaled oil recovery data for **a** chalk, **b** dolomite and **c** sandstone tests



### Development of a universal scaling equation

All the scaling equations and mathematical models proposed in the recent work (Bassir et al. 2023) and this study are shown in Table 5.

As seen in Table 5, new scaling equations and models for each lithology are not precisely the same (i.e., base literature scaling equation and model and their matching parameters). This variation proves the initial assumption of this research that the literature data must be categorized based on rock lithology. This key point must be considered in the following studies regarding scaling the spontaneous imbibition data. Each lithology has specific features (e.g., tortuosity, grains packing and sorting, etc.); therefore, the data in every study should be classified based on the rock lithology. Even carbonate categories (i.e., limestones, chalks and dolomites) have different scaling equations and mathematical models. Even though limestones and chalks are mainly composed of calcite, the difference in their grains' sorting and packing may cause a difference in their behavior and the related scaling equations and mathematical models.

All scaled oil recovery data are plotted on a log scale of 0.00001 to 100,000 for a clear comparison. The scaled recovery curves by Mattax and Kyte, Ma et al., Mason et al., limestone, chalk, dolomite and sandstone's scaling equations for all 169 tests (110 tests from this study and 59 tests from our past work (Bassir et al. 2023)) are shown in Fig. 7a–g, respectively.

The arithmetic mean of data scatter for Mattax and Kyte's, Ma et al.'s and Mason et al.'s scaling equations are 3.041, 2.911 and 2.837 log cycles, respectively. Due to the lowest value of the arithmetic mean of data scatter compared to the other scaling equations, we select Mason et al.'s scaling equation as the base equation to find a universal scaling equation for all lithologies. The new general scaling equation form is:

$$t_{D-Comprehensive} = t \sqrt{\frac{k}{\phi} \frac{\sigma}{L_c^2} \frac{2}{\mu_w + \sqrt{\mu_w \mu_o}} \left(\frac{I_w}{I_{wi}}\right)^{N_{Comprehensive}}} \tag{24}$$

An evaluation of the scaling ability of four scaling equations for each dataset compared to the best case (among three literature scaling equations) is shown in Table 6.

As can be shown from Table 6, limestone's new scaling equation [that is found based on Mason et al.'s scaling equation (Bassir et al. 2023)] has the highest scaling quality for scaling all the 169 test data compared to the other new scaling equations. This fact aligns with choosing Mason et al.'s scaling equation to improve the scaling dataset of all lithologies. A trial and error survey selects an exponent of (+0.39) with the arithmetic mean of data scatter of 2.277 log cycles, 19.7% less than Mason et al.'s scaling Eq. (2.837 log cycles). Our new proposed universal scaling equation for all lithologies is as follows:

$$t_{D-Comprehensive} = t \sqrt{\frac{k}{\phi} \frac{\sigma}{L_c^2} \frac{2}{\mu_w + \sqrt{\mu_w \mu_o}} \left(\frac{I_w}{I_{wi}}\right)^{0.39}} \tag{25}$$

The best fitted models to all the 169 scaled tests data by using Eq. (25) in Eqs. (8) and (9) are:

$$\frac{R}{R_\infty} = 1 - e^{-0.18t_{D-Comprehensive}}; RMSE = 0.195 \tag{26}$$

$$\frac{R}{R_\infty} = 1 + W(-e^{-1-0.057t_{D-Comprehensive}}); RMSE = 0.178 \tag{27}$$

As shown in Fig. 8, the Fries and Dreyer model (2008) has a lower error than the Aronofsky et al. model for fitting spontaneous imbibition oil recovery by modified salinity brine scaled by our universal scaling equation (Eq. (25)). Equation (27) can be used to develop a transfer function to predict oil recovery by the modified salinity brine in fractured reservoirs (Abouzar Mirzaei-Paيمان et al. 2011; Tavassoli et al. 2005a, b).

**Table 5** Proposed scaling equations and models for each lithology

Reference	Lithology	Number of Tests	Scaling equation	Model
Bassir et al. (2023)	Limestone	59	$t_{D-Limestone} = t \sqrt{\frac{k}{\phi} \frac{\sigma}{L_c^2} \frac{2}{\mu_w + \sqrt{\mu_w \mu_o}} \left(\frac{I_w}{I_{wi}}\right)^{0.38}}$	$\frac{R}{R_\infty} = 1 - e^{-0.24t_{D-Limestone}}$
This work	Chalk	85	$t_{D-Chalk} = t \sqrt{\frac{k}{\phi} \frac{\sigma}{L_c^2} \frac{1}{\mu_w} \left(\frac{I_w}{I_{wi}}\right)^{-1.5}}$	$\frac{R}{R_\infty} = 1 + W(-e^{-1-0.34t_{D-Chalk}})$
	Dolomite	12	$t_{D-Dolomite} = t \sqrt{\frac{k}{\phi} \frac{\sigma}{L_c^2} \frac{1}{\mu_w} \left(\frac{I_w}{I_{wi}}\right)^{0.80}}$	$\frac{R}{R_\infty} = 1 - e^{-1.6t_{D-Dolomite}}$
	Sandstone	13	$t_{D-Sandstone} = t \sqrt{\frac{k}{\phi} \frac{\sigma}{L_c^2} \frac{2}{\mu_w + \sqrt{\mu_w \mu_o}} \left(\frac{I_w}{I_{wi}}\right)^{1.5}}$	$\frac{R}{R_\infty} = 1 + W(-e^{-1-1.9t_{D-Sandstone}})$

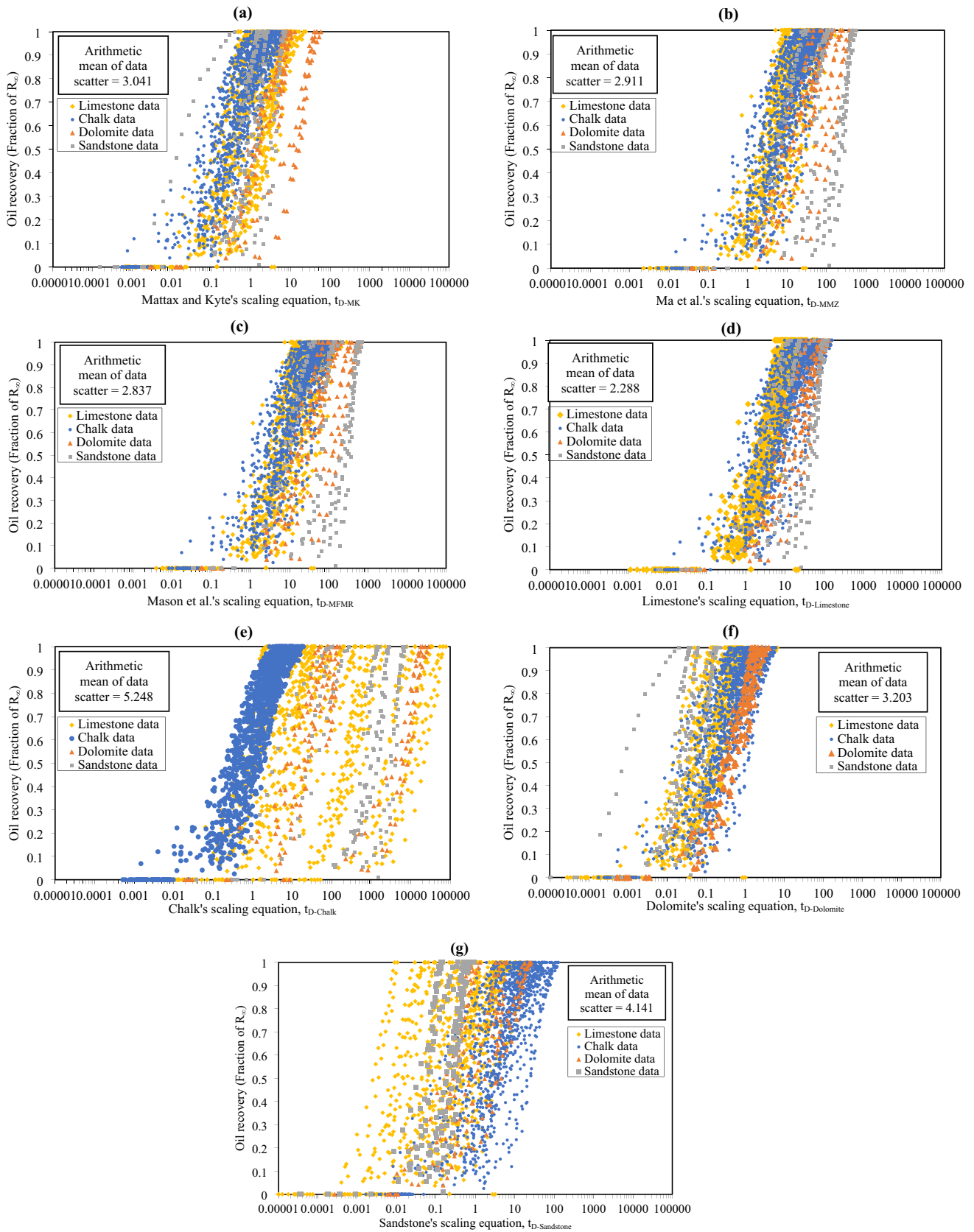


**Fig. 7** Evaluation of **a** Mattax and Kyte's, **b** Ma et al.'s, **c** Mason et al.'s, **d** limestone's, **e** chalk's, **f** dolomite's and **g** sandstone's scaling equations for all the lithologies

**Table 6** Evaluation of the scaling ability of each scaling equation for various lithologies

		$t_{D-MK}$	$t_{D-MMZ}$	$t_{D-MFMR}$	$t_{D-Limestone}$	$t_{D-Chalk}$	$t_{D-Dolomite}$	$t_{D-Sandstone}$
Limestone tests data	Arithmetic mean of data scatter	1.874	1.795	1.781	1.279	4.559	1.949	3.405
	Change percent in comparison to the best case	–	–	The best case	–28.2%	+156%	+9.43%	+91.2%
Chalk tests data	Arithmetic mean of data scatter	1.791	1.847	1.815	1.889	1.349	2.053	2.441
	Change percent in comparison to the best case	The best case	–	–	+5.47%	–24.7%	+14.6%	+36.3%
Dolomite tests data	Arithmetic mean of data scatter	1.271	1.380	1.295	0.950	3.173	0.643	1.575
	Change percent in comparison to the best case	The best case	–	–	–25.3%	+150%	–49.4%	+23.9%
Sandstone tests data	Arithmetic mean of data scatter	2.216	1.847	1.809	1.616	2.928	2.045	1.203
	Change percent in comparison to the best case	–	–	The best case	–10.7%	+61.9%	+13.0%	–33.5%
All tests data	Arithmetic mean of data scatter	3.041	2.911	2.837	2.288	5.248	3.230	4.141
	Change percent in comparison to the best case	–	–	The best case	–19.4%	+85.0%	+13.9%	+46.0%
Arithmetic mean of the change percentages					<b>–15.6%</b>	<b>+85.6%</b>	<b>+0.3%</b>	<b>+32.8%</b>

Bold row(s) indicate a conclusion from the other rows

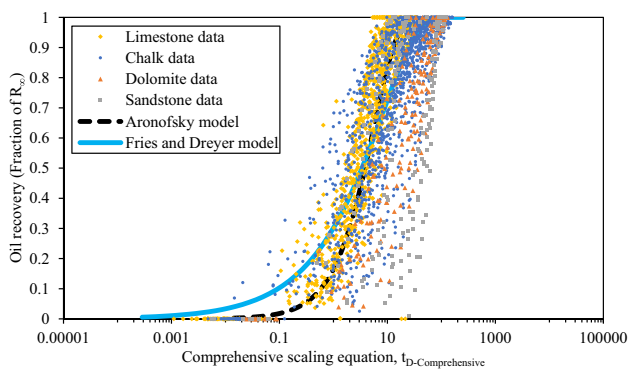


**Fig. 8** Best fitted models to the scaled oil recovery data for all the 169 gathered tests of modified salinity brine

## Recommendations for future research

For interested researchers in this research area, there is a long research road to develop scaling equations applicable to different reservoir conditions, i.e., for various EOR techniques and lithologies at reservoir conditions:

1. Many spontaneous imbibition experiments are published for water-based EOR schemes, such as surfactants (Hou et al. 2015; Santanna et al. 2014; Standnes 2004; Standnes and Austad 2000; Standnes et al. 2002) and hybrid techniques such as modified salinity brine and surfactants (Das et al. 2021; Eslahati et al. 2020; Khaleel et al. 2019; Mohammadi et al. 2019; Shi et al. 2021; Udoh and Vinogradov 2019), modified salinity brine and nanoparticles (Nowrouzi et al. 2019a; Shirazi et al. 2019) and carbonated modified

salinity brine (Amarasinghe et al. 2019; Ghandi et al. 2019; Nowrouzi et al. 2019b, 2020a, b; Nowrouzi et al. 2020a, b). Nevertheless, few scaling equations have been developed to scale these numerous tests (Keykhosravi and Simjoo 2020). Eager researchers can collect and organize the data of each EOR technique and develop proper scaling equations for each lithology.

2. For researchers interested in experimental works, it should be emphasized that many spontaneous imbibition tests with boundary conditions other than the AFO for each water-based EOR method are required.
3. Many tests with the AFO boundary condition are needed to scale hybrid EOR techniques such as carbonated modified salinity brine, modified salinity brine and nanoparticles, modified salinity brine and surfactants.
4. Applying live oil in experimental studies of spontaneous imbibition of modified salinity brine must get more attention among researchers. Scaling such data may produces more applicable scaling equations for the reservoir conditions.
5. Considering gravity force to the spontaneous imbibition scaling equations can promote their applicability in reservoir conditions. This improvement requires much more spontaneous imbibition tests on high cores. This point must be attended to in the future by interested researchers in both experimental and scaling studies.
6. The wettability alteration is the principal mechanism of most of the EOR processes. Therefore, it is recommended that the researchers report the initial and final relative permeability and capillary pressure data in their

**Table 7** Comparison of the operative ranges of the selected correlations and the gathered data

Properties Correlation / Dataset	$\gamma_o$	T (°F)	P (psia)	TAN (mgKOH/g-oil)	$C_s$ (ppm)	pH	°API
Abooli et al. (2019)	0.83-0.99	68-194	14.7-4000	0-3.7	0-300,000	6.12-8.34	
Glaso (1980)		50-300					20-48
Numbere et al. (1977)		77-302	<12,000		5800-226,100		
Chalk data	0.80-0.87	122-266	14.7	0.39-2.80	10,010-54,380	7	28.2-45.8
Dolomite data	0.85-0.88	158-194		0.14-0.92	3340-66,625		30.0-35.6
Sandstone data	0.80-0.83	122-194		0.16-1.55	966-5000		39.4-45.2

resources. These data can be applicable in the scaling equations development.

The purpose of this road may be to achieve a general scaling equation with a particular term developed for each lithology and EOR strategy.

## Conclusions

The following conclusions could be derived from this study:

1. This study presents three new empirical scaling equations to scale literature experimental recovery data of the modified salinity brine spontaneous imbibition into chalk, dolomite and sandstone rock samples. Moreover, a universal scaling equation is proposed that applies to all the lithologies (i.e., limestone, chalk, dolomite and sandstone).
2. The proposed universal scaling equation for all lithology types (169 tests) reduced the arithmetic mean of data scatter of the scaled data by 19.7% less than Mason et al.'s equation (From 2.837 to 2.277 log cycles).
3. For each lithology, a specific scaling equation is proposed. The differences in the configuration and the sign/value of matching parameters of these equations verified our basic assumption of the necessity of the classification of spontaneous imbibition experimental data based on rock lithology in the scaling studies.
4. The suggested scaling equation for chalks (85 tests) reduced the arithmetic mean of data scatter of the scaled data by 24.7% less than Mattax and Kyte's equation (From 1.791 to 1.349 log cycles).
5. The proposed scaling equation for dolomites (12 tests) declined the arithmetic mean of data scatter of the scaled data by 49.4% less than Mattax and Kyte's equation (From 1.271 to 0.643 log cycles).
6. The suggested scaling equation for sandstones (13 tests) decreased the arithmetic mean of data scatter of the scaled data by 33.5% less than Mason et al.'s equation (From 1.809 to 1.203 log cycles).
7. Four mathematical expressions (based on the Aronofsky et al. and the Fries and Dreyer models) are developed to fit the scaled imbibition recovery data by new scaling equations. These models can derive proper transfer functions for oil recovery simulation by modified salinity brine imbibition into various rocks.
8. The sign of empirical exponents of ionic strengths ratio ( $\frac{I_w}{I_{wi}}$ ) in new scaling equations shows that in dolomites and sandstones, a direct relationship is governed between the ratio of imbibing to connate brines ionic strengths ( $\frac{I_w}{I_{wi}}$ ) and the spontaneous imbibition oil recovery of modified salinity brine. Only for chalks, this relationship seems to be inverse; this discrepancy might be related to their specific porosity–permeability relationship.
9. Literature scaling equations (Mattax and Kyte's, Ma et al.'s and Mason et al.'s) could not scale the collected literature data of spontaneous imbibition of modified salinity brines. These scaling equations are for the scaling of imbibition recovery in water-wet rocks. However, Mattax and Kyte's scaling equation shows a better scaling ability of oil recovery by modified salinity brine in chalks and dolomites. In contrast, Mason et al.'s equation shows its best scaling performance for sandstones.
10. The mathematical expression based on the Aronofsky et al. model has a better fitting to scaled dolomites recovery data with lower RMSE, whereas the mathematical terms based on the Fries and Dreyer model have a better fitting to scaled chalks and sandstones recovery data with lower RMSE.

## Appendix A: Applied correlations in this research

### Abooli et al. (2019) correlation for IFT

$$\begin{aligned} \sigma = & 32.11T - 135.9\gamma_o - 3.26 \tanh(T.P.TAN) - 259.2\gamma_o^2.T \tanh(\gamma_o) - 135.9 \tanh(\gamma_o^2) + T.\gamma_o(339.1\gamma_o - 173.8) \\ & - 9.526 \tanh(T.\gamma_o.TAN^2) + 37.86 \tanh(\gamma_o + C_s) + 0.00001111T.P + \tanh(\tanh(C_s))(14.52 \tanh(P) - 30.05) \\ & - 0.1(1 + 0.1TAN.\gamma_o.pH^{0.5})(pH - 7)^2 - 0.004048TAN(1 - TAN)T + 229.73 \end{aligned} \quad (A-6)$$

where  $\sigma$ ,  $T$ ,  $P$ ,  $TAN$  and  $C_s$  are in mN/m, Kelvin (K), atmosphere (atm), milligrams of potassium hydroxide (KOH) per gram of crude oil (mgKOH/g) and ppm, respectively. Moreover,  $\gamma_o$  is the specific gravity of the crude oil (Abooli et al. 2019).

### Glaso (1980) correlation for oil viscosity

$$\mu_{od} = [3.141(10^{10})]T^{-3.444}[\log(^{\circ}\text{API})]^{10.313}[\log(T)]^{-36.447} \quad (A-1)$$

where dead oil viscosity ( $\mu_{od}$ ) and temperature ( $T$ ) are in centipoises (cp) and degrees Fahrenheit ( $^{\circ}\text{F}$ ), respectively (Glaso 1980).

### Numere et al. (1977) correlation for brine viscosity

$$\frac{\mu_w}{\mu_{pw}} - 1 = -1.87(10^{-3})C_s^{0.5} + 2.18(10^{-4})C_s^{2.5} + (T^{0.5} - 1.35(10^{-2})T)(2.76(10^{-3})C_s - 3.44(10^{-4})C_s^{1.5}) \quad (A-2)$$

where pure water viscosity ( $\mu_{pw}$ ), brine salt concentration ( $C_s$ ) and the temperature ( $T$ ) are in centipoises, weight percent (wt%) and degrees Fahrenheit ( $^{\circ}\text{F}$ ).

The  $\mu_{pw}$  at any pressure ( $P$ ) and temperature can be computed by Equation (A-3) (Numere et al. 1977):

$$\frac{\mu_{pw}(T, P)}{\mu_{pw}(T, P_s)} = 1 + \frac{P - P_s}{10^6}(1.046T - 319.24) \quad (A-3)$$

where  $P_s$  is saturation pressure in psia.

$\mu_{pw}$  at  $P_s$  and any temperature can be calculated by Equa-

tion (A-4) (Numere et al. 1977):

$$\mu_{pw}(T, P_s) = 241.4 * 10^{\left[\frac{247.8}{T-140}\right]} \quad (A-4)$$

$P_s$  can be predicted by the equation (A-5) (Numere et al. 1977):

$$P_s = 0.468\left(\frac{T}{100}\right)^{4.52} \quad (A-5)$$

See Table 7.

## Appendix B: Important properties of the literature experiments that are not included explicitly in the scaling equations

See Tables 8, 9, 10, 11, 12, 13.

**Table 8** Properties of the literature experimental data performed on chalk samples that are not included explicitly in the scaling equations

Test ID	Author(s) (Year)	Test temperature (°C)	Aging temperature (°C)	Aging time (Days)	°API	TAN (mgKOH/g)	$\frac{\mu_a}{\mu_w}$	$\mu_{wi}$ (cp)	$C_{S,w}$ (ppm)	$C_{S,wi}$ (ppm)	$\frac{I_w}{I_{wi}}$	$t_{end}$ (Days)	$R_{\infty}$ (Fractation of IOIP)
1	Zhang and Austad (2006)	70	90	30	44.7	0.55	1.96	0.477	33,390	82,050	0.452	30	0.28
2		70	90	30	44.7	0.55	1.96	0.477	34,190	82,050	0.452	29	0.17
3		70	90	30	44.7	0.55	1.96	0.477	34,190	82,050	0.452	29	0.14
4		100	90	28	44.1	2.07	2.06	0.337	33,390	82,050	0.452	25	0.27
5		100	90	28	44.1	2.07	2.07	0.337	31,790	82,050	0.452	31	0.44
6		100	90	28	44.1	2.07	2.07	0.337	31,790	82,050	0.452	31	0.18
7		100	90	28	44.1	2.07	2.07	0.337	32,590	82,050	0.452	31	0.33
8		100	90	28	44.1	2.07	2.07	0.337	30,990	82,050	0.452	31	0.50
9		100	90	28	44.1	2.07	2.06	0.337	34,190	82,050	0.452	5	0.09
10		130	90	57	44.1	2.07	2.06	0.258	32,590	82,050	0.452	4	0.65
11		130	90	57	44.1	2.07	2.06	0.258	33,390	82,050	0.452	8	0.58
12		130	90	57	44.1	2.07	2.06	0.258	31,790	82,050	0.452	10	0.43
13		130	90	57	44.1	2.07	2.06	0.258	32,590	82,050	0.452	5	0.59
14	Zhang et al. (2006)	100	90	42	44.1	2.07	2.07	0.312	30,900	47,455	0.647	45	0.16
15		70	90	42	44.1	2.07	2.07	0.463	33,400	68,000	0.452	27	0.24
16		100	90	42	44.1	2.07	2.06	0.315	33,400	51,176	0.615	45	0.15
17		70	90	42	44.1	2.07	2.07	0.463	34,000	68,000	0.452	12	0.09
18		100	90	30	44.1	2.07	2.07	0.327	30,900	68,000	0.452	13	0.29
19		130	90	30	44.1	2.07	2.07	0.241	30,900	52,368	0.587	11	0.14
20		100	90	30	44.1	2.07	2.06	0.327	33,400	68,000	0.452	7	0.24
21		130	90	30	44.1	2.07	2.06	0.242	33,400	54,212	0.578	25	0.34
22		100	90	30	44.1	2.07	2.06	0.327	34,000	68,000	0.452	18	0.22
23		130	90	30	44.1	2.07	2.05	0.243	34,000	55,534	0.566	25	0.28
24		130	90	30	44.1	2.07	2.05	0.250	33,800	68,000	0.452	14	0.62
25		130	90	30	44.1	2.07	2.07	0.250	30,900	68,000	0.452	11	0.60
26		130	90	30	44.1	2.07	2.06	0.250	33,400	68,000	0.452	11	0.57
27		70	90	30	44.7	0.55	1.97	0.463	32,600	68,000	0.452	30	0.45
28		70	90	30	44.7	0.55	1.96	0.463	33,400	68,000	0.452	30	0.38
29		70	90	30	44.7	0.55	1.96	0.477	33,400	82,100	0.452	30	0.28
30		70	90	30	44.7	0.55	1.96	0.463	34,000	68,000	0.452	29	0.28
31		70	90	30	44.7	0.55	1.96	0.477	34,000	82,100	0.452	29	0.17

Table 8 (continued)

Test ID	Author(s) (Year)	Test temperature (°C)	Aging temperature (°C)	Aging time (Days)	°API	TAN (mgKOH/g)	$\frac{\mu_a}{\mu_w}$	$\mu_{vi}$ (cp)	$C_{S,w}$ (ppm)	$C_{S,vi}$ (ppm)	$\frac{I_w}{I_{vi}}$	$t_{end}$ (Days)	$R_{\infty}$ (Fraction of IOIP)
32	Zhang et al. (2007)	100	90	42	44.1	2.07	2.04	0.329	38,397	71,005	0.608	30	0.21
33		130	90	42	44.1	2.07	2.03	0.246	38,397	61,966	0.682	21	0.27
34		100	90	42	44.1	2.07	2.04	0.329	39,196	71,413	0.607	31	0.10
35		130	90	42	44.1	2.07	2.03	0.249	39,196	66,560	0.645	15	0.06
36		100	90	42	44.1	2.07	2.05	0.328	37,025	70,053	0.561	21	0.14
37		130	90	42	44.1	2.07	2.04	0.247	37,025	62,872	0.620	15	0.05
38		100	90	42	44.1	2.07	2.05	0.328	36,000	69,604	0.617	31	0.32
39		130	90	42	44.1	2.07	2.04	0.244	36,000	57,221	0.718	21	0.31
40		70	90	42	44.7	0.55	1.96	0.453	34,930	57,550	0.641	15	0.28
41		70	90	42	44.7	0.55	1.96	0.464	34,230	69,613	0.530	13	0.14
42		70	90	42	44.1	2.07	2.06	0.469	36,210	74,142	0.497	14	0.07
43		70	90	42	44.1	2.07	2.07	0.465	34,930	70,502	0.522	13	0.03
44		100	90	42	44.1	2.07	2.06	0.328	34,930	69,145	0.532	13	0.16
45	130	90	42	44.1	2.07	2.05	0.248	34,930	64,220	0.570	8	0.11	
46	70	90	42	44.1	2.07	2.06	0.467	35,820	72,507	0.508	14	0.03	
47	100	90	42	44.1	2.07	2.06	0.328	34,230	70,191	0.525	13	0.12	
48	130	90	42	44.1	2.07	2.05	0.248	34,230	64,245	0.569	14	0.32	
49	Strand et al. (2008)	120	90	28	45.4	1.90	1.88	0.259	33,419	46,847	0.760	35	0.22
50		50	90	28	44.9	0.39	1.87	0.616	54,380	62,800	0.886	78	0.28
51	Puntervold et al. (2009)	50	90	28	44.9	0.39	1.89	0.616	49,180	62,800	0.813	78	0.36
52		50	90	28	44.9	0.39	1.93	0.616	36,890	62,800	0.639	78	0.27
53		70	90	28	44.9	0.45	1.92	0.458	36,890	62,800	0.639	40	0.51
54		70	90	28	44.9	0.69	1.87	0.458	49,180	62,800	0.813	91	0.36
55		70	90	28	44.9	0.69	1.92	0.458	36,890	62,800	0.639	91	0.31
56		90	90	28	44.9	0.69	1.85	0.359	54,380	62,800	0.886	78	0.40
57		90	90	28	44.9	0.69	1.87	0.359	49,180	62,800	0.813	47	0.35
58		90	90	28	44.9	0.69	1.92	0.359	36,890	62,800	0.639	70	0.34
59		110	90	28	44.9	0.70	1.87	0.293	49,180	62,800	0.813	35	0.57
60		110	90	28	44.9	0.70	1.89	0.293	43,910	62,800	0.738	38	0.60
61	110	90	28	44.9	0.70	1.92	0.293	36,890	62,800	0.639	41	0.61	
62	130	90	28	44.9	1.10	1.87	0.247	49,180	62,800	0.813	35	0.68	
63	130	90	28	44.9	1.10	1.92	0.247	36,890	62,800	0.639	35	0.63	

Table 8 (continued)

Test ID	Author(s) (Year)	Test temperature (°C)	Aging temperature (°C)	Aging time (Days)	°API	TAN (mgKOH/g)	$\frac{\mu_a}{\mu_w}$	$\mu_{vi}$ (cp)	$C_{S,w}$ (ppm)	$C_{S,vi}$ (ppm)	$\frac{I_w}{I_{vi}}$	$t_{end}$ (Days)	$R_{\infty}$ (Fraction of IOIP)
64	Fathi et al. (2010a)	100	90	28	42.9	1.90	2.26	0.323	33,390	62,800	0.591	49	0.41
65		110	90	28	42.9	1.90	2.25	0.293	33,390	62,800	0.591	56	0.47
66		120	90	28	42.9	1.90	2.38	0.268	10,010	62,800	0.231	22	0.70
67		120	90	28	42.9	1.90	2.24	0.268	33,390	62,800	0.591	28	0.62
68	Fathi et al. (2010b)	110	90	28	42.8	1.80	2.27	0.282	33,400	44,512	0.789	57	0.34
69		110	90	28	42.8	1.80	2.27	0.281	33,400	42,992	0.812	57	0.37
70		110	90	28	42.3	1.50	2.34	0.280	33,400	41,823	0.831	57	0.46
71		110	90	28	42.3	1.50	2.34	0.280	33,400	41,940	0.829	57	0.45
72	Fathi et al. (2011a)	110	90	28	43.3	1.90	2.18	0.283	33,400	46,673	0.759	36	0.24
73		110	90	28	43.3	1.90	2.18	0.282	33,400	45,918	0.769	30	0.26
74		110	90	28	43.5	1.90	2.15	0.281	33,400	44,185	0.794	64	0.35
75		110	90	28	43.5	1.90	2.15	0.281	33,400	44,124	0.795	64	0.41
76	Fathi et al. (2011b)	70	90	28	45.8	0.50	1.86	0.458	16,790	62,800	0.425	27	0.49
77		70	90	28	45.8	0.50	1.89	0.458	10,010	62,800	0.231	25	0.45
78		90	90	28	45.8	0.50	1.88	0.359	16,790	62,800	0.425	37	0.62
79		90	90	28	45.8	0.50	1.81	0.359	33,390	62,800	0.591	37	0.38
80		100	90	56	42.1	2.00	2.52	0.323	11,430	62,800	0.331	12	0.10
81		100	90	56	42.1	2.00	2.53	0.323	10,010	62,800	0.231	9	0.11
82		120	90	56	42.1	2.00	2.47	0.268	16,790	62,800	0.425	52	0.48
83	Kazankapov (2014)	90	90	28	28.2	2.80	10.90	0.359	10,010	62,800	0.231	37	0.46
84		90	90	28	28.2	2.80	10.73	0.359	16,790	62,800	0.425	34	0.62
85		90	90	28	28.2	2.80	10.34	0.359	33,390	62,800	0.591	34	0.38
Minimum		<b>50</b>	<b>90</b>	<b>28</b>	<b>28.2</b>	<b>0.39</b>	<b>1.81</b>	<b>0.241</b>	<b>10,010</b>	<b>41,823</b>	<b>0.231</b>	<b>4</b>	<b>0.03</b>
Arithmetic mean		<b>99</b>	<b>90</b>	<b>34</b>	<b>43.6</b>	<b>1.57</b>	<b>2.35</b>	<b>0.348</b>	<b>33,441</b>	<b>65,174</b>	<b>0.567</b>	<b>32</b>	<b>0.34</b>
Maximum		<b>130</b>	<b>90</b>	<b>57</b>	<b>45.8</b>	<b>2.80</b>	<b>10.90</b>	<b>0.616</b>	<b>54,380</b>	<b>82,100</b>	<b>0.886</b>	<b>91</b>	<b>0.70</b>

Bold row(s) indicate a conclusion from the other rows



**Table 9** Properties of the literature experimental data performed on dolomite samples that are not included explicitly in the scaling equations

Test ID	Author(s) (Year)	Test temperature (°C)	Aging temperature (°C)	Aging time (Days)	°API	TAN (mgKOH/g)	$\frac{\mu_a}{\mu_w}$	$\mu_{wi}$ (cp)	$C_{s,w}$ (ppm)	$C_{s,at}$ (ppm)	$\frac{I_w}{I_{wi}}$	$t_{end}$ (Days)	$R_{\infty}$ (Fractation of IOIP)
1	Romanuka et al. (2012)	70	85	28	30.0	0.92	9.0	0.703	33,390	220,373	0.152	5	0.02
2		70	85	28	30.0	0.92	9.6	0.668	3340	205,068	0.017	34	0.15
3		70	85	28	30.0	0.92	9.0	0.703	33,390	220,373	0.152	6	0.01
4		70	85	28	30.0	0.92	9.6	0.676	3340	209,001	0.017	28	0.10
5	Shariatpanahi et al. (2016)	70	70	21	35.6	0.52	4.6	0.707	33,430	222,190	0.150	6	0.01
6		70	70	21	35.6	0.52	4.9	0.685	3343	212,929	0.016	28	0.10
7		70	70	21	35.6	0.52	4.6	0.707	33,430	222,190	0.150	5	0.02
8		70	70	21	35.6	0.52	4.9	0.675	3343	208,513	0.016	33	0.15
9	Mehraban et al. (2020)	90	90	40	31.3	0.14	6.6	0.500	57,647	189,412	0.235	38	0.35
10		90	90	40	31.3	0.14	6.6	0.500	60,308	189,412	0.251	36	0.38
11		90	90	40	31.3	0.14	6.7	0.500	48,088	189,412	0.228	31	0.44
12		90	90	40	31.3	0.14	6.5	0.500	66,625	189,412	0.287	26	0.39
Minimum		<b>70</b>	<b>70</b>	<b>21</b>	<b>30.0</b>	<b>0.14</b>	<b>4.6</b>	<b>0.500</b>	<b>3340</b>	<b>189,412</b>	<b>0.016</b>	<b>5</b>	<b>0.01</b>
Arithmetic mean		<b>77</b>	<b>82</b>	<b>30</b>	<b>32.3</b>	<b>0.53</b>	<b>6.9</b>	<b>0.627</b>	<b>31,640</b>	<b>206,524</b>	<b>0.139</b>	<b>23</b>	<b>0.18</b>
Maximum		<b>90</b>	<b>90</b>	<b>40</b>	<b>35.6</b>	<b>0.92</b>	<b>9.6</b>	<b>0.707</b>	<b>66,625</b>	<b>222,190</b>	<b>0.287</b>	<b>38</b>	<b>0.44</b>

Bold row(s) indicate a conclusion from the other rows

**Table 10** Properties of the literature experimental data performed on sandstone samples that are not included explicitly in the scaling equations

Test ID	Authors (Year)	Test temperature (°C)	Aging temperature (°C)	Aging time (Days)	°API	TAN (mgKOH/g)	$\frac{\mu_o}{\mu_w}$	$\mu_{vir}$ (cp)	$C_{s,0}$ (ppm)	$C_{s,0}$ (ppm)	$\frac{L_w}{L_{wi}}$	$t_{end}$ (Days)	$R_{co}$ (Fraction of IOIP)
1	Yang et al. (2016)	60	60	14	45.2	1.30	4.3	0.489	1000	25,000	0.040	4.0	0.07
2		60	60	14	45.2	1.30	4.3	0.479	1000	14,178	0.070	3.3	0.04
3	Shehata and Nasr-El-Din (2017)	66	85	20	39.4	0.92	15.2	0.639	5000	174,156	0.025	25.0	0.64
4	Al-Saedi et al. (2019)	90	90	21	42.1	0.66	2.6	0.390	1182	100,000	0.009	15.0	0.30
5		90	90	21	42.1	0.66	2.6	0.390	1182	100,000	0.009	15.0	0.18
6		90	90	21	42.1	0.66	2.6	0.390	1182	100,000	0.009	15.0	0.11
7		90	90	21	42.1	0.66	2.6	0.390	1182	100,000	0.009	14.0	0.09
8	Al-Saedi et al. (2020)	50	90	42	41.1	1.55	3.0	0.673	966	104,550	0.010	40.0	0.12
9		50	90	42	41.1	1.55	3.0	0.673	966	104,550	0.010	40.0	0.10
10		50	90	42	41.1	0.16	3.0	0.673	966	104,550	0.010	41.0	0.44
11		50	90	42	41.1	0.16	3.0	0.673	966	104,550	0.010	32.0	0.38
12		50	90	42	41.1	0.90	3.0	0.673	966	104,550	0.010	36.0	0.24
13		50	90	42	41.1	0.90	3.0	0.673	966	104,550	0.010	37.0	0.20
Minimum		<b>50</b>	<b>60</b>	<b>14</b>	<b>39.4</b>	<b>0.16</b>	<b>2.6</b>	<b>0.390</b>	<b>966</b>	<b>14,178</b>	<b>0.009</b>	<b>3.3</b>	<b>0.04</b>
Arithmetic mean		<b>65</b>	<b>85</b>	<b>30</b>	<b>41.9</b>	<b>0.88</b>	<b>4.0</b>	<b>0.554</b>	<b>1348</b>	<b>95,433</b>	<b>0.018</b>	<b>24.4</b>	<b>0.22</b>
Maximum		<b>90</b>	<b>90</b>	<b>42</b>	<b>45.2</b>	<b>1.55</b>	<b>15.2</b>	<b>0.673</b>	<b>5000</b>	<b>174,156</b>	<b>0.070</b>	<b>41.0</b>	<b>0.64</b>

Bold row(s) indicate a conclusion from the other rows

**Table 11** Ionic compositions of applied brines in the chalk tests

Test ID	Author(s) (Year)	Imbibing brine				Connate brine			
		Sodium (ppm)	Chlorine (ppm)	Mag-nesium (ppm)	Sulfate (ppm)	Sodium (ppm)	Chlorine (ppm)	Mag-nesium (ppm)	Sulfate (ppm)
1	Zhang and Austad (2006)	10,350	18,719	1094	2305	30,797	50,131	608	0
2		10,764	20,527	1094	576	30,797	50,131	608	0
3		10,902	21,165	1094	0	30,797	50,131	608	0
4		10,350	18,719	1094	2305	30,797	50,131	608	0
5		9246	13,508	1094	6916	30,797	50,131	608	0
6		10,626	19,889	1094	1153	30,797	50,131	608	0
7		9798	16,060	1094	4611	30,797	50,131	608	0
8		8694	10,955	1094	9222	30,797	50,131	608	0
9		10,902	21,165	1094	0	30,797	50,131	608	0
10		9798	16,060	1094	4611	30,797	50,131	608	0
11		10,350	18,719	1094	2305	30,797	50,131	608	0
12		10,626	19,889	1094	1153	30,797	50,131	608	0
13		9798	16,060	1094	4611	30,797	50,131	608	0
14	Zhang et al. (2006)	7659	17,230	1094	2305	11,324	28,658	873	1259
15		10,350	18,719	1094	2305	15,732	42,402	608	0
16		10,350	18,719	1094	2305	13,146	31,021	841	1108
17		11,247	19,074	1094	0	15,732	42,402	608	0
18		7659	17,230	1094	2305	15,732	42,402	608	0
19		7659	17,230	1094	2305	12,378	31,944	810	958
20		10,350	18,719	1094	2305	15,732	42,402	608	0
21		10,350	18,719	1094	2305	13,612	33,075	799	908
22		11,247	19,074	1094	0	15,732	42,402	608	0
23		11,247	19,074	1094	0	14,101	33,919	784	838
24		10,810	18,861	1094	240	15,732	42,402	608	0
25		7659	17,230	1094	2305	15,732	42,402	608	0
26		10,350	18,719	1094	2305	15,732	42,402	608	0
27		9798	16,060	1094	4611	15,732	42,402	608	0
28		10,350	18,719	1094	2305	15,732	42,402	608	0
29		10,350	18,719	1094	2305	30,797	50,131	608	0
30		10,764	20,527	1094	576	15,732	42,402	608	0
31		10,764	20,527	1094	576	30,797	50,131	608	0

Table 11 (continued)

Test ID	Author(s) (Year)	Imbibing brine					Connate brine				
		Sodium (ppm)	Chlorine (ppm)	Mag- nesium (ppm)	Calcium (ppm)	Sulfate (ppm)	Sodium (ppm)	Chlorine (ppm)	Mag- nesium (ppm)	Calcium (ppm)	Sulfate (ppm)
32	Zhang et al. (2007)	14,329	20,669	1094	0	2305	27,837	42,496	0	0	672
33		14,329	20,669	1094	0	2305	24,093	36,445	303	0	1125
34		14,881	23,222	1094	0	0	28,067	43,346	0	0	0
35		14,881	23,222	1094	0	0	26,081	40,314	165	0	0
36		13,777	18,116	0	521	4611	27,385	41,256	0	0	1413
37		13,777	18,116	0	521	4611	24,426	36,225	0	113	2108
38		12,673	13,011	1094	0	9222	27,166	40,627	0	0	1811
39		12,673	13,011	1094	0	9222	21,826	30,451	403	0	4542
40		11,247	19,074	0	1783	2305	21,357	34,058	278	625	1232
41		11,247	19,074	1082	0	2305	25,813	42,000	452	736	612
42		12,627	19,783	0	986	2305	27,447	44,980	500	838	377
43		11,247	19,074	0	1783	2305	26,043	42,594	453	852	560
44		11,247	19,074	0	1783	2305	25,487	41,710	436	887	626
45		11,247	19,074	0	1783	2305	23,468	38,500	374	1014	864
46		12,627	19,783	598	0	2305	26,864	43,901	478	801	463
47		11,247	19,074	1082	0	2305	25,971	42,402	489	751	577
48		11,247	19,074	1082	0	2305	23,571	38,600	586	629	859
49	Strand et al. (2008)	10,350	18,613	1094	521	2305	16,367	27,786	664	828	1203
50	Puntervold et al. (2009)	19,182	32,085	486	1002	768	22,908	37,793	194	1162	0
51		16,974	28,752	632	882	1153	22,908	37,793	194	1162	0
52		11,822	20,882	997	601	2017	22,908	37,793	194	1162	0
53		11,822	20,882	997	601	2017	22,908	37,793	194	1162	0
54		16,974	28,752	632	882	1153	22,908	37,793	194	1162	0
55		11,822	20,882	997	601	2017	22,908	37,793	194	1162	0
56		19,182	32,085	486	1002	768	22,908	37,793	194	1162	0
57		16,974	28,752	632	882	1153	22,908	37,793	194	1162	0
58		11,822	20,882	997	601	2017	22,908	37,793	194	1162	0
59		16,974	28,752	632	882	1153	22,908	37,793	194	1162	0
60		14,766	25,349	778	761	1537	22,908	37,793	194	1162	0
61		11,822	20,882	997	601	2017	22,908	37,793	194	1162	0
62		16,974	28,752	632	882	1153	22,908	37,793	194	1162	0
63		11,822	20,882	997	601	2017	22,908	37,793	194	1162	0

Table 11 (continued)

Test ID	Author(s) (Year)	Imbibing brine				Connate brine					
		Sodium (ppm)	Chlorine (ppm)	Mag-nesium (ppm)	Calcium (ppm)	Sulfate (ppm)	Sodium (ppm)	Chlorine (ppm)	Mag-nesium (ppm)	Calcium (ppm)	Sulfate (ppm)
64	Fathi et al. (2010a)	10,350	18,613	1094	521	2305	23,000	37,935	194	1162	0
65		10,350	18,613	1094	521	2305	23,000	37,935	194	1162	0
66		1150	4467	1094	521	2305	23,000	37,935	194	1162	0
67		10,350	18,613	1094	521	2305	23,000	37,935	194	1162	0
68	Fathi et al. (2010b)	10,350	18,613	1094	521	2305	15,356	26,258	735	777	1387
69		10,350	18,613	1094	521	2305	14,701	25,259	782	743	1507
70		10,350	18,613	1094	521	2305	14,198	24,490	818	718	1599
71		10,350	18,613	1094	521	2305	14,248	24,567	815	720	1590
72	Fathi et al. (2011a)	10,350	18,613	1094	521	2305	16,286	27,679	669	824	1216
73		10,350	18,613	1094	521	2305	15,961	27,182	692	808	1275
74		10,350	18,613	1094	521	2305	15,215	26,043	745	769	1412
75		10,350	18,613	1094	521	2305	15,188	26,003	747	768	1417
76	Fathi et al. (2011b)	4462	4467	1094	521	9222	23,000	37,935	194	1162	0
77		1150	4467	1094	521	2305	23,000	37,935	194	1162	0
78		4462	4467	1094	521	9222	23,000	37,935	194	1162	0
79		10,350	18,613	1094	521	2305	23,000	37,935	194	1162	0
80		1150	6842	1094	2084	2305	23,000	37,935	194	1162	0
81		1150	4467	1094	521	2305	23,000	37,935	194	1162	0
82		4462	4467	1094	521	9222	23,000	37,935	194	1162	0
83	Kazankapov (2014)	1150	4467	1094	521	2305	23,000	37,935	194	1162	0
84		4462	4467	1094	521	9222	23,000	37,935	194	1162	0
85		10,350	18,613	1094	521	2305	23,000	37,935	194	1162	0
Minimum		<b>1150</b>	<b>4467</b>	<b>0</b>	<b>0</b>	<b>0</b>	<b>11,324</b>	<b>24,490</b>	<b>0</b>	<b>0</b>	<b>0</b>
Arithmetic mean		<b>10,634</b>	<b>18,229</b>	<b>945</b>	<b>636</b>	<b>2762</b>	<b>22,502</b>	<b>39,439</b>	<b>435</b>	<b>2174</b>	<b>418</b>
Maximum		<b>19,182</b>	<b>32,085</b>	<b>1094</b>	<b>2084</b>	<b>9222</b>	<b>30,797</b>	<b>50,131</b>	<b>873</b>	<b>9258</b>	<b>4542</b>

Bold row(s) indicate a conclusion from the other rows

**Table 12** Ionic compositions of applied brines in the dolomite tests

Test ID	Author(s) (Year)	Imbibing brine					Connate brine				
		Sodium (ppm)	Chlorine (ppm)	Magnesium (ppm)	Calcium (ppm)	Sulfate (ppm)	Sodium (ppm)	Chlorine (ppm)	Magnesium (ppm)	Calcium (ppm)	Sulfate (ppm)
1	Romanuka	10,350	18,613	1094	521	2305	64,929	136,423	2236	16,592	192
2	et al. (2012)	1035	1861	109	52	230	60,420	126,948	2081	15,440	179
3		10,350	18,613	1094	521	2305	64,929	136,423	2236	16,592	192
4		1035	1861	109	52	230	61,579	129,383	2121	15,736	182
5	Shariatpanahi	10,350	18,648	1094	521	2305	65,527	137,097	2236	16,592	192
6	et al. (2016)	1035	1865	109	52	230	62,979	131,627	2183	15,850	290
7		10,350	18,648	1094	521	2305	65,527	137,097	2236	16,592	192
8		1035	1865	109	52	230	61,688	128,856	2157	15,474	339
9	Mehraban	27	42,448	14,019	660	0	56,993	113,672	660	14,548	1750
10	et al. (2020)	1481	41,280	14,019	0	3035	56,993	113,672	660	14,548	1750
11		5824	21,998	7010	660	12,105	56,993	113,672	660	14,548	1750
12		2935	42,448	14,019	660	6071	56,993	113,672	660	14,548	1750
Minimum		<b>27</b>	<b>1861</b>	<b>109</b>	<b>0</b>	<b>0</b>	<b>56,993</b>	<b>113,672</b>	<b>660</b>	<b>14,548</b>	<b>179</b>
Arithmetic mean		<b>4651</b>	<b>19,179</b>	<b>4490</b>	<b>356</b>	<b>2613</b>	<b>61,296</b>	<b>126,545</b>	<b>1677</b>	<b>15,589</b>	<b>730</b>
Maximum		<b>10,350</b>	<b>42,448</b>	<b>14,019</b>	<b>660</b>	<b>12,105</b>	<b>65,527</b>	<b>137,097</b>	<b>2236</b>	<b>16,592</b>	<b>1750</b>

Bold row(s) indicate a conclusion from the other rows

**Table 13** Ionic compositions of applied brines in the sandstone tests

Test ID	Author(s) (Year)	Imbibing brine					Connate brine				
		Sodium (ppm)	Chlorine (ppm)	Magnesium (ppm)	Calcium (ppm)	Sulfate (ppm)	Sodium (ppm)	Chlorine (ppm)	Magnesium (ppm)	Calcium (ppm)	Sulfate (ppm)
1	Yang et al. (2016)	0	638	0	361	0	0	15,954	0	9018	0
2		0	638	0	361	0	0	9058	0	5120	0
3	Shehata and Nasr-El-Din (2017)	1967	3033	0	0	0	54,400	107,000	1610	10,600	370
4	Al-Saedi et al. (2019)	384	585	0	0	0	34,500	58,497	2163	0	0
5		384	585	0	0	0	34,500	58,497	4326	0	0
6		384	585	0	0	0	34,500	58,497	0	3567	0
7		384	585	0	0	0	34,500	58,497	0	7134	0
8	Al-Saedi et al. (2020)	266	565	62	11	62	31,656	64,278	1021	7222	372
9		266	565	62	11	62	31,656	64,278	1021	7222	372
10		266	565	62	11	62	31,656	64,278	1021	7222	372
11		266	565	62	11	62	31,656	64,278	1021	7222	372
12		266	565	62	11	62	31,656	64,278	1021	7222	372
13		266	565	62	11	62	31,656	64,278	1021	7222	372
Minimum		<b>0</b>	<b>565</b>	<b>0</b>	<b>0</b>	<b>0</b>	<b>0</b>	<b>9058</b>	<b>0</b>	<b>0</b>	<b>0</b>
Arithmetic mean		<b>392</b>	<b>772</b>	<b>29</b>	<b>61</b>	<b>28</b>	<b>29,411</b>	<b>57,821</b>	<b>1094</b>	<b>6059</b>	<b>200</b>
Maximum		<b>1967</b>	<b>3033</b>	<b>62</b>	<b>361</b>	<b>62</b>	<b>54,400</b>	<b>107,000</b>	<b>4326</b>	<b>10,600</b>	<b>372</b>

Bold row(s) indicate a conclusion from the other rows

**Funding** This work is not funded directly or indirectly by any organization.

## Declarations

**Conflict of interest** On behalf of all the co-authors, the corresponding authors state that there is no conflict of interest.

**Ethical approval** In this research, there are no funding, potential conflicts of interest (financial or non-financial), and informed consent.

**Open Access** This article is licensed under a Creative Commons Attribution 4.0 International License, which permits use, sharing, adaptation, distribution and reproduction in any medium or format, as long as you give appropriate credit to the original author(s) and the source, provide a link to the Creative Commons licence, and indicate if changes were made. The images or other third party material in this article are included in the article's Creative Commons licence, unless indicated otherwise in a credit line to the material. If material is not included in the article's Creative Commons licence and your intended use is not permitted by statutory regulation or exceeds the permitted use, you will need to obtain permission directly from the copyright holder. To view a copy of this licence, visit <http://creativecommons.org/licenses/by/4.0/>.

## References

- Aadnoy BS, Looyeh R (2019) Petroleum rock mechanics: drilling operations and well design. Gulf Professional Publishing
- Abooali D, Sobati MA, Shahhosseini S, Assareh M (2019) A new empirical model for estimation of crude oil/brine interfacial tension using genetic programming approach. *J Pet Sci Eng* 173:187–196. <https://doi.org/10.1016/j.petrol.2018.09.073>
- Al-Saedi HN, Al-Jaberi SK, Flori RE, Al-Bazzaz W (2020) Novel Insights into low salinity water flooding enhanced oil recovery in sandstone: the role of calcite. Paper presented at the SPE improved oil recovery conference. <https://doi.org/10.2118/200444-MS>
- Al-Saedi HN, Flori RE, Brady PV (2019) Effect of divalent cations in formation water on wettability alteration during low salinity water flooding in sandstone reservoirs: oil recovery analyses, surface reactivity tests, contact angle, and spontaneous imbibition experiments. *J Mol Liq* 275:163–172. <https://doi.org/10.1016/j.molliq.2018.11.093>
- Amarasinghe W, Fjelde I, Guo Y, Chauhan J (2019) Visualization of spontaneous imbibition of carbonated water at different permeability and wettability conditions. Paper presented at the IOR 2019–20th European symposium on improved oil recovery. <https://doi.org/10.3997/2214-4609.201900177>
- Anderson W (1986) Wettability literature survey-part 2: wettability measurement. *J Pet Technol* 38(11):1246–1262. <https://doi.org/10.2118/13933-PA>
- Aronofsky JS, Masse L, Natanson SG (1958) A model for the mechanism of oil recovery from the porous matrix due to water invasion in fractured reservoirs. *Trans AIME* 213(1):17–19. <https://doi.org/10.2118/932-G>
- Bassir SM, Shadzadeh SR (2020) Static adsorption of a new cationic biosurfactant on carbonate minerals: application to EOR. *Pet Sci Technol* 38(5):462–471. <https://doi.org/10.1080/10916466.2020.1727922>
- Bassir SM, Shokrollahzadeh Behbahani H, Shahbazi K, Kord S, Mirzaei-Paiaman A (2023) Towards prediction of oil recovery by spontaneous imbibition of modified salinity brine into limestone rocks: a scaling study. *J Pet Explor Product Technol* 13(1):79–99. <https://doi.org/10.1007/s13202-022-01537-7>
- Behbahani HS, Blunt MJ (2005) Analysis of imbibition in mixed-wet rocks using pore-scale modeling. *SPE J* 10(4):466–474. <https://doi.org/10.2118/90132-PA>
- Behbahani HS, Di Donato G, Blunt MJ (2006) Simulation of counter-current imbibition in water-wet fractured reservoirs. *J Pet Sci Eng* 50(1):21–39. <https://doi.org/10.1016/j.petrol.2005.08.001>
- Cai J, Hu X, Standnes DC, You L (2012) An analytical model for spontaneous imbibition in fractal porous media including gravity. *Colloids Surf A* 414:228–233. <https://doi.org/10.1016/j.colsurfa.2012.08.047>
- Cai J, Yu B, Zou M, Luo L (2010) Fractal characterization of spontaneous co-current imbibition in porous media. *Energy Fuels* 24(3):1860–1867. <https://doi.org/10.1021/ef901413p>
- Chandrasekhar S, Mohanty K (2013) Wettability alteration with brine composition in high temperature carbonate reservoirs. Paper presented at the SPE annual technical conference and exhibition. <https://doi.org/10.2118/166280-MS>
- Das S, Katiyar A, Rohilla N, Bonnecaze RT, Nguyen Q (2021) A methodology for chemical formulation for wettability alteration induced water imbibition in carbonate reservoirs. *J Pet Sci Eng* 198:108–136. <https://doi.org/10.1016/j.petrol.2020.108136>
- Eslahati M, Mehrabianfar P, Isari AA, Bahramnejad H, Manshad AK, Keshavarz A (2020) Experimental investigation of Alfalfa natural surfactant and synergistic effects of  $\text{Ca}^{2+}$ ,  $\text{Mg}^{2+}$ , and  $\text{SO}_4^{2-}$  ions for EOR applications: Interfacial tension optimization, wettability alteration and imbibition studies. *J Mol Liq* 310:113–123. <https://doi.org/10.1016/j.molliq.2020.113123>
- Fathi SJ, Austad T, Strand S (2010a) “Smart water” as a wettability modifier in chalk: the effect of salinity and ionic composition. *Energy Fuels* 24(4):2514–2519. <https://doi.org/10.1021/ef901304m>
- Fathi SJ, Austad T, Strand S (2011a) Effect of water-extractable carboxylic acids in crude oil on wettability in carbonates. *Energy Fuels* 25(6):2587–2592. <https://doi.org/10.1021/ef200302d>
- Fathi SJ, Austad T, Strand S (2011b) Water-based enhanced oil recovery (EOR) by “smart water”: optimal ionic composition for EOR in carbonates. *Energy Fuels* 25(11):5173–5179. <https://doi.org/10.1021/ef201019k>
- Fathi SJ, Austad T, Strand S, Puntervold T (2010b) Wettability alteration in carbonates: the effect of water-soluble carboxylic acids in crude oil. *Energy Fuels* 24(5):2974–2979. <https://doi.org/10.1021/ef901527h>
- Fischer H, Morrow NR (2006) Scaling of oil recovery by spontaneous imbibition for wide variation in aqueous phase viscosity with glycerol as the viscosifying agent. *J Pet Sci Eng* 52(1–4):35–53
- Fischer H, Wo S, Morrow NR (2008) Modeling the effect of viscosity ratio on spontaneous imbibition. Paper presented at the SPE annual technical conference and exhibition. <https://doi.org/10.2118/102641-MS>
- Fries N, Dreyer M (2008) An analytic solution of capillary rise restrained by gravity. *J Colloid Interface Sci* 320(1):259–263. <https://doi.org/10.1016/j.jcis.2008.01.009>
- Ghandi E, Parsaei R, Riazi M (2019) Enhancing the spontaneous imbibition rate of water in oil-wet dolomite rocks through boosting a wettability alteration process using carbonated smart brines. *Pet Sci* 16(6):1361–1373. <https://doi.org/10.1007/s12182-019-0355-1>
- Gilman JR, Kazemi H (1983) Improvements in simulation of naturally fractured reservoirs. *Soc Pet Eng J* 23(4):695–707. <https://doi.org/10.2118/10511-PA>
- Glaso O (1980) Generalized pressure-volume-temperature correlations. *J Pet Technol* 32(5):785–795. <https://doi.org/10.2118/8016-PA>
- Hamon G, Vidal J (1986) Scaling-up the capillary imbibition process from laboratory experiments on homogeneous and heterogeneous samples. In: SPE Europec featured at EAGE Conference and Exhibition. SPE, pp. SPE-15852



- Hatiboglu CU, Babadagli T (2004) Dynamics of spontaneous counter-current imbibition for different matrix shape factors, interfacial tensions, wettabilities and oil types. Paper presented at the Canadian international petroleum conference. <https://doi.org/10.2118/2004-091>
- Hatiboglu CU, Babadagli T (2006) Primary and secondary oil recovery from different-wettability rocks by countercurrent diffusion and spontaneous imbibition. Paper presented at the SPE/DOE symposium on improved oil recovery. <https://doi.org/10.2118/94120-PA>
- Hou B-F, Wang Y-F, Huang Y (2015) Study of spontaneous imbibition of water by oil-wet sandstone cores using different surfactants. *J Dispers Sci Technol* 36(9):1264–1273. <https://doi.org/10.1080/01932691.2014.971808>
- Hückel E, Debye P (1923) The theory of electrolytes: I. Lowering of freezing point and related phenomena. *Phys Z* 24(1):185–206
- Kazankapov N (2014) Enhanced oil recovery in Caspian carbonates with Smart Water. Paper presented at the SPE Russian oil and gas exploration and production technical conference and exhibition. <https://doi.org/10.2118/171258-MS>
- Kazemi H, Gilman JR, Elsharkawy A (1992) Analytical and numerical solution of oil recovery from fractured reservoirs with empirical transfer functions. *SPE Reserv Eng J* 7(2):219–227. <https://doi.org/10.2118/19849-PA>
- Keykhosravi A, Simjoo M (2020) Enhancement of capillary imbibition by Gamma-Alumina nanoparticles in carbonate rocks: underlying mechanisms and scaling analysis. *J Pet Sci Eng* 187:106802. <https://doi.org/10.1016/j.petrol.2019.106802>
- Khaleel O, Teklu TW, Alameri W, Abass H, Kazemi H (2019) Wettability alteration of carbonate reservoir cores—laboratory evaluation using complementary techniques. *SPE Reserv Eval Eng* 22(3):911–922. <https://doi.org/10.2118/194483-PA>
- Li K, Horne RN (2005) Computation of capillary pressure and global mobility from spontaneous water imbibition into oil-saturated rock. *SPE J* 10(4):458–465. <https://doi.org/10.2118/80553-PA>
- Li K, Horne RN (2006) Generalized scaling approach for spontaneous imbibition: an analytical model. *SPE Reserv Eval Eng* 9(3):251–258. <https://doi.org/10.2118/77544-PA>
- Ligthelm DJ, Gronsveld J, Hofman J, Brussee N, Marcelis F, van der Linde H (2009) Novel waterflooding strategy by manipulation of injection brine composition. Paper presented at the EURO-PEC/EAGE conference and exhibition. <https://doi.org/10.2118/119835-MS>
- Ma S, Morrow NR, Zhang X (1995) Generalized scaling of spontaneous imbibition data for strongly water-wet systems. Paper presented at the Technical Meeting/Petroleum Conference of The South Saskatchewan Section
- Ma S, Morrow NR, Zhang X (1997) Generalized scaling of spontaneous imbibition data for strongly water-wet systems. *J Pet Sci Eng* 18(3–4):165–178. [https://doi.org/10.1016/S0920-4105\(97\)00020-X](https://doi.org/10.1016/S0920-4105(97)00020-X)
- Madsen L, Ida L (1998) Adsorption of carboxylic acids on reservoir minerals from organic and aqueous phase. *SPE Reserv Eval Eng* 1(1):47–51. <https://doi.org/10.2118/37292-PA>
- Mahani H, Keya AL, Berg S, Bartels W-B, Nasralla R, Rossen WR (2015) Insights into the mechanism of wettability alteration by low-salinity flooding (LSF) in carbonates. *Energy Fuels* 29(3):1352–1367. <https://doi.org/10.1021/ef5023847>
- Mahzari P, Sohrabi M, Façanha JM (2019) The decisive role of microdispersion formation in improved oil recovery by low-salinity-water injection in sandstone formations. *SPE J* 24(06):2859–2873. <https://doi.org/10.2118/197067-PA>
- Mandal A (2015) Chemical flood enhanced oil recovery: a review. *Int J Oil Gas Coal Technol* 9(3):241–264. <https://doi.org/10.1504/IJOGCT.2015.069001>
- Mason G, Fischer H, Morrow N, Ruth D (2010) Correlation for the effect of fluid viscosities on counter-current spontaneous imbibition. *J Pet Sci Eng* 72(1–2):195–205. <https://doi.org/10.1016/j.petrol.2010.03.017>
- Mattax CC, Kyte J (1962) Imbibition oil recovery from fractured, water-drive reservoir. *Soc Pet Eng J* 2(2):177–184. <https://doi.org/10.2118/187-PA>
- Mehraban MF, Rostami P, Afzali S, Ahmadi Z, Sharifi M, Ayatollahi S (2020) Brine composition effect on the oil recovery in carbonate oil reservoirs: a comprehensive experimental and CFD simulation study. *J Pet Sci Eng* 191:107–149. <https://doi.org/10.1016/j.petrol.2020.107149>
- Mirzaei-Paiaman A (2015) Analysis of counter-current spontaneous imbibition in presence of resistive gravity forces: displacement characteristics and scaling. *J Unconv Oil Gas Resour* 12:68–86. <https://doi.org/10.1016/j.juogr.2015.09.001>
- Mirzaei-Paiaman A, Kord S, Hamidpour E, Mohammadzadeh O (2017) Scaling one- and multi-dimensional co-current spontaneous imbibition processes in fractured reservoirs. *Fuel* 196:458–472. <https://doi.org/10.1016/j.fuel.2017.01.120>
- Mirzaei-Paiaman A, Masihi M, Standnes DC (2011) An analytic solution for the frontal flow period in 1D counter-current spontaneous imbibition into fractured porous media including gravity and wettability effects. *Transp Porous Media* 89(1):49–62. <https://doi.org/10.1007/s11242-011-9751-8>
- Mirzaei-Paiaman A, Masihi M (2014) Scaling of recovery by cocurrent spontaneous imbibition in fractured petroleum reservoirs. *Energy Technol* 2(2):166–175. <https://doi.org/10.1002/ente.201300155>
- Mohammadi S, Kord S, Moghadasi J (2019) An experimental investigation into the spontaneous imbibition of surfactant assisted low salinity water in carbonate rocks. *Fuel* 243:142–154. <https://doi.org/10.1016/j.fuel.2019.01.074>
- Mohammadkhani S, Shahverdi H, Esfahany MN (2018) Impact of salinity and connate water on low salinity water injection in secondary and tertiary stages for enhanced oil recovery in carbonate oil reservoirs. *J Geophys Eng* 15(4):1242–1254. <https://doi.org/10.1088/1742-2140/aaae84>
- Nowrouzi I, Manshad AK, Mohammadi AH (2019a) Effects of concentration and size of TiO<sub>2</sub> nano-particles on the performance of smart water in wettability alteration and oil production under spontaneous imbibition. *J Pet Sci Eng* 183:106357. <https://doi.org/10.1016/j.petrol.2019.106357>
- Nowrouzi I, Manshad AK, Mohammadi AH (2019b) Effects of ions and dissolved carbon dioxide in brine on wettability alteration, contact angle and oil production in smart water and carbonated smart water injection processes in carbonate oil reservoirs. *Fuel* 235:1039–1051. <https://doi.org/10.1016/j.fuel.2018.08.067>
- Nowrouzi I, Manshad AK, Mohammadi AH (2020a) The mutual effects of injected fluid and rock during imbibition in the process of low and high salinity carbonated water injection into carbonate oil reservoirs. *J Mol Liq* 305:112432. <https://doi.org/10.1016/j.molliq.2019.112432>
- Nowrouzi I, Mohammadi AH, Manshad AK (2020b) Effects of methanol and acetone as mutual solvents on wettability alteration of carbonate reservoir rock and imbibition of carbonated seawater. *J Pet Sci Eng* 195:107609. <https://doi.org/10.1016/j.petrol.2020.107609>
- Numbers D, Brigham WE, Standing M (1977) Correlations for physical properties of petroleum reservoir brines. Stanford Univ., CA (USA). Petroleum Research Inst.
- Pooladi-Darvish M, Firoozabadi A (2000a) Cocurrent and counter-current imbibition in a water-wet matrix block. *SPE J* 5(1):3–11. <https://doi.org/10.2118/38443-PA>
- Pooladi-Darvish M, Firoozabadi A (2000b) Experiments and modelling of water injection in water-wet fractured porous media. *J Can Pet Technol* 39(3):31–42. <https://doi.org/10.2118/00-03-02>

- Punternvold T, Strand S, Austad T (2007) Water flooding of carbonate reservoirs: effects of a model base and natural crude oil bases on chalk wettability. *Energy Fuels* 21(3):1606–1616. <https://doi.org/10.1021/ef060624b>
- Punternvold T, Strand S, Austad T (2009) Coinjection of seawater and produced water to improve oil recovery from fractured North Sea chalk oil reservoirs. *Energy Fuels* 23(5):2527–2536. <https://doi.org/10.1021/ef801023u>
- Rapoport L (1955) Scaling laws for use in design and operation of water-oil flow models. *Trans AIME* 204(1):143–150. <https://doi.org/10.2118/415-G>
- Romanuka J, Hofman J, Ligthelm DJ, Suijkerbuijk B, Marcelis A, Oedai S, Brussee NJ, van der Linde A, Aksulu H, Austad T (2012) Low salinity EOR in carbonates. Paper presented at the SPE improved oil recovery symposium. <https://doi.org/10.2118/153869-MS>
- Roostaei A (2014) Enhanced oil recovery (EOR) by "smart water" in carbonates reservoir. MS Thesis, University of Stavanger, Norway
- Saidi AM (1987) Reservoir engineering of fractured reservoirs (fundamental and Practical Aspects). Total
- Salih TA, Sahi SH, AL-Dujaili ANG (2016) Using different surfactants to increase oil recovery of Rumaila field (Experimental Work). *Iraqi J Chem Pet Eng* 17(3):11–31. <https://doi.org/10.31699/IJCPPE.2016.3.2>
- Santanna V, Castro Dantas T, Borges T, Bezerril A, Nascimento A (2014) The influence of surfactant solution injection in oil recovery by spontaneous imbibition. *Pet Sci Technol* 32(23):2896–2902. <https://doi.org/10.1080/10916466.2014.921200>
- Schmid K, Geiger S (2012) Universal scaling of spontaneous imbibition for water-wet systems. *Water Resour Res*. <https://doi.org/10.1029/2011WR011566>
- Schmid K, Geiger S (2013) Universal scaling of spontaneous imbibition for arbitrary petrophysical properties: water-wet and mixed-wet states and Handy's conjecture. *J Pet Sci Eng* 101:44–61. <https://doi.org/10.1016/j.petrol.2012.11.015>
- Shariatpanahi S, Hopkins P, Aksulu H, Strand S, Punternvold T, Austad T (2016) Water based EOR by wettability alteration in dolomite. *Energy Fuels* 30(1):180–187. <https://doi.org/10.1021/acs.energyfuels.5b02239>
- Shariatpanahi SF, Strand S, Austad T (2010) Evaluation of water-based enhanced oil recovery (EOR) by wettability alteration in a low-permeable fractured limestone oil reservoir. *Energy Fuels* 24(11):5997–6008. <https://doi.org/10.1021/ef100837v>
- Sharma M, Filoco P (2000) Effect of brine salinity and crude-oil properties on oil recovery and residual saturations. *SPE J* 5(3):293–300. <https://doi.org/10.2118/65402-PA>
- Shehata AM, Nasr-El-Din HA (2017) Laboratory investigations to determine the effect of connate-water composition on low-salinity waterflooding in sandstone reservoirs. *SPE Reserv Eval Eng* 20(1):59–76. <https://doi.org/10.2118/171690-PA>
- Shi Y, Miller C, Mohanty K (2021) Surfactant-aided low-salinity waterflooding for low-temperature carbonate reservoirs. *SPE J* 26(4):2214–2230. <https://doi.org/10.2118/201754-PA>
- Shirazi M, Farzaneh J, Kord S, Tamsilian Y (2020) Smart water spontaneous imbibition into oil-wet carbonate reservoir cores: symbiotic and individual behavior of potential determining ions. *J Mol Liq* 299:112102. <https://doi.org/10.1016/j.molliq.2019.112102>
- Shirazi M, Kord S, Tamsilian Y (2019) Novel smart water-based titania nanofluid for enhanced oil recovery. *J Mol Liq* 296:112064. <https://doi.org/10.1016/j.molliq.2019.112064>
- Skauge A, Standal S, Boe S, Skauge T, Blokhus A (1999) Effects of organic acids and bases, and oil composition on wettability. Paper presented at the SPE annual technical conference and exhibition. <https://doi.org/10.2118/56673-MS>
- Standnes DC (2004) Analysis of oil recovery rates for spontaneous imbibition of aqueous surfactant solutions into preferential oil-wet carbonates by estimation of capillary diffusivity coefficients. *Colloids Surf A* 251(1–3):93–101. <https://doi.org/10.1016/j.colsurfa.2004.09.013>
- Standnes DC (2010) A single-parameter fit correlation for estimation of oil recovery from fractured water-wet reservoirs. *J Pet Sci Eng* 71(1–2):19–22. <https://doi.org/10.1016/j.petrol.2009.12.008>
- Standnes DC, PIØ A (2017) Analysis of the impact of fluid viscosities on the rate of countercurrent spontaneous imbibition. *Energy Fuels* 31(7):6928–6940. <https://doi.org/10.1021/acs.energyfuels.7b00863>
- Standnes DC, Austad T (2000) Wettability alteration in chalk: 2. Mechanism for wettability alteration from oil-wet to water-wet using surfactants. *J Pet Sci Eng* 28(3):123–143. [https://doi.org/10.1016/S0920-4105\(00\)00084-X](https://doi.org/10.1016/S0920-4105(00)00084-X)
- Standnes DC, Nogaret LA, Chen H-L, Austad T (2002) An evaluation of spontaneous imbibition of water into oil-wet carbonate reservoir cores using a nonionic and a cationic surfactant. *Energy Fuels* 16(6):1557–1564. <https://doi.org/10.1021/ef0201127>
- Strand S, Punternvold T, Austad T (2008) Effect of temperature on enhanced oil recovery from mixed-wet chalk cores by spontaneous imbibition and forced displacement using seawater. *Energy Fuels* 22(5):3222–3225. <https://doi.org/10.1021/ef800244v>
- Strand S, Standnes DC, Austad T (2003) Spontaneous imbibition of aqueous surfactant solutions into neutral to oil-wet carbonate cores: effects of brine salinity and composition. *Energy Fuels* 17(5):1133–1144. <https://doi.org/10.1021/ef030051s>
- Tavassoli Z, Zimmerman RW, Blunt MJ (2005a) Analysis of countercurrent imbibition with gravity in weakly water-wet systems. *J Pet Sci Eng* 48(1–2):94–104. <https://doi.org/10.1016/j.petrol.2005.04.003>
- Tavassoli Z, Zimmerman RW, Blunt MJ (2005b) Analytic analysis for oil recovery during counter-current imbibition in strongly water-wet systems. *Transp Porous Media* 58(1):173–189. <https://doi.org/10.1007/s11242-004-5474-4>
- Udoh T, Vinogradov J (2019) A synergy between controlled salinity brine and biosurfactant flooding for improved oil recovery: an experimental investigation based on zeta potential and interfacial tension measurements. *Int J Geophys*. <https://doi.org/10.1155/2019/2495614>
- van Golf-Racht TD (1982) Fundamentals of fractured reservoir engineering. Elsevier
- Warren J, Root PJ (1963) The behavior of naturally fractured reservoirs. *Soc Pet Eng J* 3(3):245–255. <https://doi.org/10.2118/426-PA>
- Yang J, Dong Z, Dong M, Yang Z, Lin M, Zhang J, Chen C (2016) Wettability alteration during low-salinity waterflooding and the relevance of divalent ions in this process. *Energy Fuels* 30(1):72–79. <https://doi.org/10.1021/acs.energyfuels.5b01847>
- Zhang P, Austad T (2006) Wettability and oil recovery from carbonates: effects of temperature and potential determining ions. *Colloids Surf A* 279(1–3):179–187. <https://doi.org/10.1016/j.colsurfa.2006.01.009>
- Zhang P, Tweheyo MT, Austad T (2006) Wettability alteration and improved oil recovery in chalk: the effect of calcium in the presence of sulfate. *Energy Fuels* 20(5):2056–2062. <https://doi.org/10.1021/ef0600816>
- Zhang P, Tweheyo MT, Austad T (2007) Wettability alteration and improved oil recovery by spontaneous imbibition of seawater into chalk: impact of the potential determining ions  $\text{Ca}^{2+}$ ,  $\text{Mg}^{2+}$ , and  $\text{SO}_4^{2-}$ . *Colloids Surf A* 301(1–3):199–208. <https://doi.org/10.1016/j.colsurfa.2006.12.058>

Zhang X, Morrow NR, Ma S (1996) Experimental verification of a modified scaling group for spontaneous imbibition. SPE Reserv Eng J 11(4):280–285. <https://doi.org/10.2118/30762-PA>

Zhou D, Jia L, Kamath J, Kovsky A (2002) Scaling of counter-current imbibition processes in low-permeability porous media. J Pet Sci

Eng 33(1–3):61–74. [https://doi.org/10.1016/S0920-4105\(01\)00176-0](https://doi.org/10.1016/S0920-4105(01)00176-0)

**Publisher's Note** Springer Nature remains neutral with regard to jurisdictional claims in published maps and institutional affiliations.